

Several mechanisms drive the heterogeneity in browning across a boreal stream network

Xudan Zhu¹, Frank Berninger¹, Liang Chen¹, Johannes Larson², Ryan Sponseller³, and Hjalmar Laudon⁴

¹University of Eastern Finland

²Swedish University of Agricultural Science

³Umeå University

⁴Swedish University of Agricultural Sciences

December 10, 2023

Abstract

Increases in dissolved organic carbon (DOC) have occurred in many freshwaters across Europe and North America over the last decades. Several mechanisms have been proposed to explain these trends, but consensus regarding the relative importance of recovery from acid deposition, climate change, and land management remains elusive. To advance our understanding of browning mechanisms, we explored DOC trends across 13 nested boreal catchments, leveraging concurrent hydrological, chemical, and terrestrial ecosystem data to quantify the contributions of different drivers on observed trends. We first identified the environmental factors related to DOC concentrations, then attributed the individual trends of DOC to potential drivers across space and time. The results showed that all catchments exhibited increased DOC trends from 2003 to 2021, but the DOC response rates differed five-fold. No single mechanism can fully explain the ongoing browning, instead the interaction of sulfate deposition, climate-related factors and site properties jointly controlled the variation in DOC trends. Specifically, the long-term increases in DOC were primarily driven by recovery from sulfate deposition, followed by terrestrial productivity, temperature, and discharge. However, catchment size and landcover type regulated the response rate of DOC trends to these drivers, creating the spatial heterogeneity in browning among the sub-catchments under similar deposition and climate forcing. Interestingly, browning has weakened in the last decade as sulfate deposition has fully recovered and other current drivers are insufficient to sustain the long-term trends. Our results highlight that multifaceted, spatially structured, and nonstationary drivers must be accounted for to predict future browning.

Hosted file

980662_0_art_file_11647621_s4zrgm.docx available at <https://authorea.com/users/707188/articles/692221-several-mechanisms-drive-the-heterogeneity-in-browning-across-a-boreal-stream-network>



1
2 **Several mechanisms drive the heterogeneity in browning**
3 **across a boreal stream network**

4 **Xudan Zhu^{1*}, Frank Berninger¹, Liang Chen¹, Johannes Larson², Ryan A. Sponseller³,**
5 **Hjalmar Laudon²**

6 ¹ Department of Environmental and Biological Sciences, Joensuu Campus, University of Eastern
7 Finland, 80100 Joensuu, Finland.

8 ² Department of Forest Ecology and Management, Swedish University of Agricultural Science,
9 90183 Umeå, Sweden.

10 ³ Department of Ecology and Environmental Sciences, Umeå University, 901 87 Umeå, Sweden.

11 * ORCID: 0000-0002-8540-384X. Address: *Natura 372 a, Yliopistokatu 2, FI-80100 Joensuu,*
12 *Finland.* Phone: +358408279940

13 Corresponding author: Xudan Zhu (xudanzhu@uef.fi).

14 **Key Points:**

- 15 • This study evaluated the multiple mechanisms behind browning using a 19-year time
16 series data across 13 nested boreal catchments.
- 17 • We revealed recovery from sulfate, rather than from acidification per se, as the primary
18 driver of browning despite low deposition history.
- 19 • Our results provided an explanation for spatiotemporal heterogeneity of browning trends
20 within a boreal catchment network.

Abstract

23 Increases in dissolved organic carbon (DOC) have occurred in many freshwaters across Europe
24 and North America over the last decades. Several mechanisms have been proposed to explain
25 these trends, but consensus regarding the relative importance of recovery from acid deposition,
26 climate change, and land management remains elusive. To advance our understanding of
27 browning mechanisms, we explored DOC trends across 13 nested boreal catchments, leveraging
28 concurrent hydrological, chemical, and terrestrial ecosystem data to quantify the contributions of
29 different drivers on observed trends. We first identified the environmental factors related to DOC
30 concentrations, then attributed the individual trends of DOC to potential drivers across space and
31 time. The results showed that all catchments exhibited increased DOC trends from 2003 to 2021,
32 but the DOC response rates differed five-fold. No single mechanism can fully explain the
33 ongoing browning, instead the interaction of sulfate deposition, climate-related factors and site
34 properties jointly controlled the variation in DOC trends. Specifically, the long-term increases in
35 DOC were primarily driven by recovery from sulfate deposition, followed by terrestrial
36 productivity, temperature, and discharge. However, catchment size and landcover type regulated
37 the response rate of DOC trends to these drivers, creating the spatial heterogeneity in browning
38 among the sub-catchments under similar deposition and climate forcing. Interestingly, browning
39 has weakened in the last decade as sulfate deposition has fully recovered and other current
40 drivers are insufficient to sustain the long-term trends. Our results highlight that multifaceted,
41 spatially structured, and nonstationary drivers must be accounted for to predict future browning.

42

43

44 **Plain Language Summary**

45 In recent decades, many lakes and rivers in Europe and North America have seen a rise in
46 dissolved organic carbon (DOC), giving the water brownish color. Researchers have suggested
47 different reasons for this, like recovery from acid rain, climate change, and landuse change, yet
48 we're not sure which is the most important. To better understand, we looked at DOC changes in
49 13 nested rivers, considering all possible causes. We found that all rivers had an increase in DOC
50 from 2003 to 2021, but the increase varied among the rivers. The main drivers of long-term
51 increases in DOC were recovery from sulfate deposition, followed by increased plant biomass,
52 temperature, and water flow. The size of river and land cover type of surroundings also affected
53 how quickly DOC levels changed. Strikingly, browning has slowed down in the last 10 years
54 with total recovery from sulfate deposition, while other factors are too weak to keep browning
55 going. Our study shows that we need to consider multiple environmental factors that vary over
56 space and time to predict DOC trends in the future.

57

58

59

60

61

62

63

64 **1 Introduction**

65 The flux of dissolved organic carbon (DOC) from terrestrial to aquatic ecosystems is an
66 important aspect of the global carbon (C) cycle (Aitkenhead & McDowell, 2000), with far-
67 reaching consequences for the chemistry, biology, and ecology of streams, rivers, and lakes
68 (Driscoll et al., 1988; Karlsson et al., 2009; Martell et al., 1988). Globally, riverine DOC fluxes
69 account for approximately 25-50% of the total C exports to oceans (Cole et al., 2007; Ciais et al.,
70 2008; Drake et al., 2018). Yet, over the last few decades, many catchments in Europe and North
71 America have witnessed rising DOC concentrations in surface waters, often termed “browning”
72 (Monteith et al., 2007; Clark et al., 2010; Lawrence & Roy, 2021). Increases in water color
73 caused by elevated DOC supply affects light penetration and thermal regimes that can further
74 alter the biodiversity and food webs of aquatic ecosystems (Conley et al., 2011; Leach et al.,
75 2019; Kritzberg et al., 2020). Further, increasing DOC reduces the value of aquatic landscapes
76 from the recreational and aesthetic aspects and boosts the cost of purifying drinking water
77 (Blanchet et al., 2022).

78 Several mechanisms have been proposed to explain the rising DOC concentration, including
79 recovery from atmospheric acid deposition, climate change, land use alteration, and increases in
80 terrestrial productivity (Kritzberg et al. 2020). Indeed, recovery from acid deposition after its
81 peak in the 1970s is a well-established driver of browning, with reductions in acidity and ionic
82 strength of soil water increasing the solubility of DOC and thus its potential for lateral export
83 (Monteith et al., 2007; Pagano et al., 2014; Lawrence & Roy, 2021). There is also mounting
84 evidence that land-use changes drive increases in aquatic DOC, either by enhancing terrestrial
85 organic C accumulation or by altering DOC routing from soils to streams (Kritzberg, 2017;
86 Härkönen et al., 2023). Finally, a range of climate change-related factors, including increased

87 temperature (Keller et al., 2008), altered hydrology (Tiwari et al., 2022), and elevated
88 atmospheric CO₂ (Schlesinger & Andrews, 2000), along with a longer growing season and higher
89 productivity (Finstad et al., 2016), have also been suggested as drivers of browning. Collectively,
90 these factors must be linked to enhanced organic matter pools on land, but also to elevated rates
91 of soil C decomposition, shifts in hydrological pathways, and reduced travel time of DOC in
92 aquatic networks (Tranvik & Jansson, 2002; Hongve et al., 2004). Of these, connections between
93 ongoing increases in terrestrial productivity (Myers-Smith et al., 2020) and elevated DOC export
94 have gained some of the most recent interest (Larsen et al., 2011; Finstad et al., 2016; Mzobe et
95 al., 2018), and could be particularly important in regions not exposed to high rates of acid
96 deposition or major land use changes. Yet, while recent research supports the role of terrestrial
97 productivity in controlling DOC concentrations in boreal catchments (Zhu et al., 2022), the
98 relationship between terrestrial greening and aquatic browning is not well established.
99 Ultimately, a major challenge to understanding the mechanisms behind browning is that several
100 of these drivers can co-occur, may be interactive, and shift in importance over time. Thus,
101 resolving amongst them requires time series data that simultaneously capture chemical,
102 hydrological, and terrestrial ecosystem parameters, but also new analytical tools that can isolate
103 potentially non-stationary causal connections.

104 Some differences in the suggested drivers of browning across studies may be caused by spatial
105 variation in historical acid deposition (Clark et al., 2010). For example, at regional scales,
106 variable deposition history may determine the potential for other factors, including climate
107 warming and changes in hydrology, to drive DOC increases (Räike et al., 2016). However, even
108 closely co-located streams, with similar deposition history, can exhibit different DOC trends
109 (Fork et al., 2020), suggesting that local catchment properties can mediate responses to broader-

110 scale drivers. In boreal landscapes, small-scale differences in mire (wetlands) versus forest cover
111 appear to play this role, with DOC trends being far stronger in forest-dominated compared to
112 mire-dominated streams (Fork et al., 2020). The mechanistic basis for these patterns remains
113 unresolved but such distinct DOC trends suggest fundamental differences in how different land
114 covers mediate the response to historical acid inputs. In addition, Zhu et al., (2022) found that
115 terrestrial productivity promotes DOC production in small forested catchments via priming, a
116 process that may underpin some of the differences in DOC trends between forest- mire-
117 dominated catchments. Finally, moving beyond headwater systems, increases in catchment size
118 can lead to greater supplies of deep, DOC-poor groundwater (Tiwari et al., 2018), and these
119 inputs may regulate and/or dampen DOC trends for larger streams and rivers (Zhu et al., 2022).
120 Overall, while broad-scale environmental changes are clearly influencing DOC production and
121 supply from catchment soils, predicting the browning trend in river networks also requires that
122 we consider the role of catchment size and landscape modulating factors.

123 In addition to recognizing spatial drivers, differences in the temporal scales considered may also
124 give rise to a change in responsible drivers of browning, particularly in reference to the pace of
125 acid deposition recovery. Based on the long-term monitoring programs in the northern
126 hemisphere, most regions have shown continued browning trends (Redden et al., 2021; Lapierre
127 et al., 2021; Lepistö et al., 2021). Wit et al., (2016) observed positive trends of DOC in 474
128 boreal and subarctic catchments across Europe from 1990 to 2013, even suggesting that the
129 future changes in precipitation are likely to promote continued browning. Conversely, Eklöf et
130 al., (2021) proposed that the widespread increases in DOC concentration across Sweden ceased a
131 decade ago due to full recovery from acidification. These contrasting findings cast doubt on the
132 hypothesis that ongoing pressures, such as climate change, are driving widespread browning.

133 Therefore, understanding the relative contributions of all the proposed mechanisms on different
134 spatiotemporal scales remains critical for generating accurate predictions about the future
135 browning trends.

136 To address the open questions on the heterogeneity of browning in a river network, we ask how
137 DOC trends in a northern boreal stream network relate to concurrent changes in sulfur (S)
138 deposition recovery and climate-related factors and how these relationships are mediated by
139 variability in catchment size and land cover. We answered these questions using two decades of
140 monitoring data from the Krycklan Catchment Study, located in northern Sweden. Krycklan is
141 comprised of multiple, nested sub-catchments that encompass the natural variability in land
142 cover features (e.g., forest and mire cover) typical of the region, as well as a wide range of
143 catchment sizes. Additionally, it is an area with comparatively low S deposition historically,
144 while the streams are naturally acidic, anthropogenic acidity has been restricted to hydrological
145 episodes during snowmelt (Laudon, Sponseller, et al., 2021). To investigate the trends in DOC
146 concentrations and identify potential drivers across the 13 nested boreal catchments experiencing
147 similar climate and S deposition history, we pursued the following objectives:

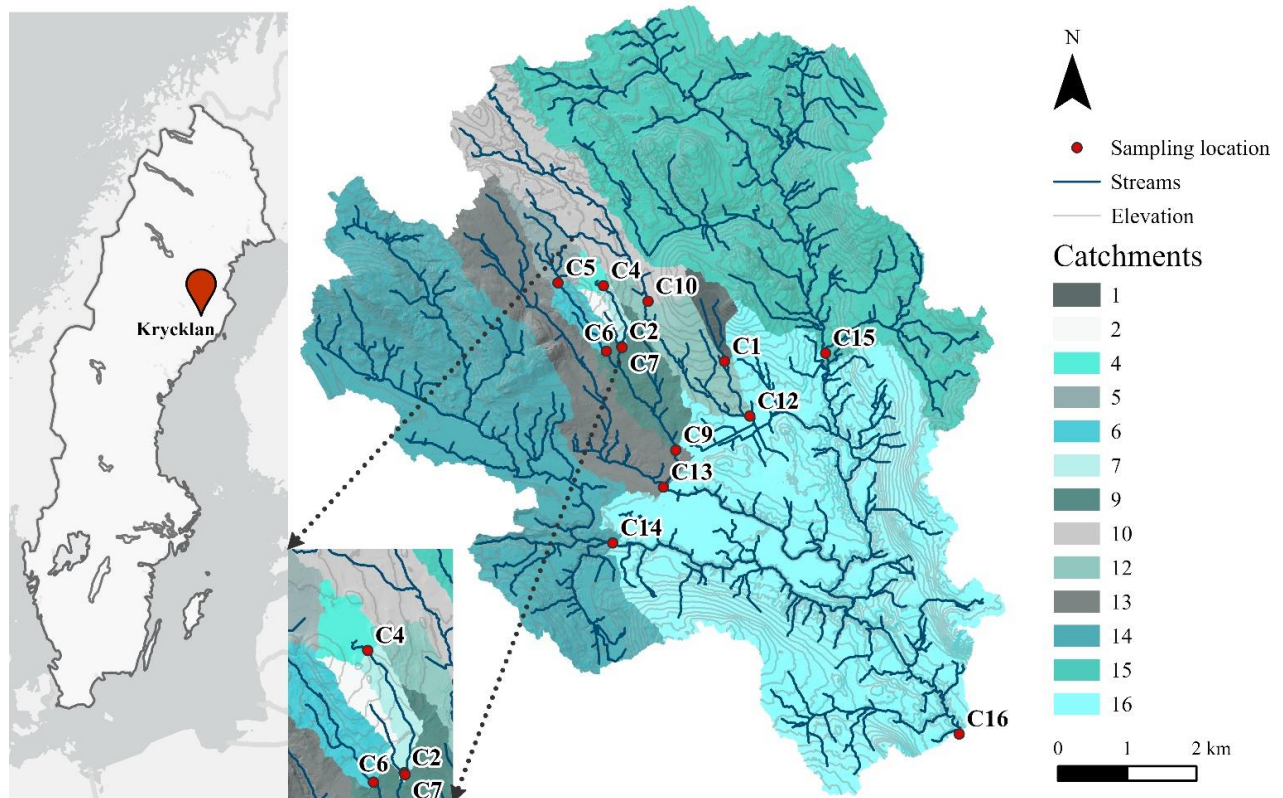
- 148 1. To develop empirical models based on different mechanisms, including climate change
149 and recovery from S deposition, as well as site characteristics including catchment size
150 and land cover type. These models aim to reveal the underlying drivers of DOC trends.
- 151 2. To quantify the contributions of the identified drivers to the long-term trends of DOC
152 from both spatial and temporal perspectives. This step aims to provide a comprehensive
153 understanding of the factors controlling the spatiotemporal heterogeneity in long-term
154 DOC trends across boreal catchments.

155 **2. Materials and Methods**

156 2.1 Study area

157 Krycklan is located in the boreal landscape, approximately 50 km northwest of the city of Umeå
 158 in northern Sweden ($64^{\circ} 14'N$, $19^{\circ}46'E$) (Figure 1). This study investigated 13 long-term
 159 monitoring catchments in Krycklan with varied sizes from 12 to 6790 ha, and landscape types
 160 dominated by both forest and mires (Table 1). For 10 of the 13 catchments, the measurement
 161 period was from 2003 to 2021, but from 2003 to 2018 for C12, C14, and C15.

162



163

164

Figure 1. Nested catchments, sampling locations and study sites in Krycklan, Sweden

165 Underlying bedrock in the catchment consists of 94% metasediments/metagraywacke, 4% acid
 166 and intermediate metavolcanic rocks, and 3% basic metavolcanic rocks. Above the highest
 167 postglacial coastline across Krycklan (257 m a.s.l), glacial till dominates quaternary deposits,
 168 while post-glacial sedimentary deposits dominate soils below it (Laudon et al., 2013). Forests
 169 cover 87% of the area and are predominantly Scots pine (*Pinus sylvestris*, 63%), and Norway
 170 spruce (*Picea abies*, 26%) with 9% deciduous forest. Peatlands cover 9% of the catchment and
 171 are dominated by *Sphagnum* species. The climate is characterized as a cold temperate humid
 172 type with persistent snow cover during winter. The 30-year mean annual average precipitation
 173 (1981-2010) is 614 mm of which 35% was classified as snow during winter (December to April),
 174 annual runoff is 311 mm, giving annual average evapotranspiration of 303 mm. The mean annual
 175 temperature is 1.8 °C, January -9.5°C and July +14.7 °C. The average snow water equivalent for
 176 the last 40 years of record is 180 mm, ranging from 64 (1996) to 321 (1988) mm. The 40-year
 177 average duration of winter snow cover is 167 days (Laudon, Hasselquist, et al., 2021).

178 Table 1. Catchment properties of all catchments in this study

Properties	Unit	C1	C2	C4	C5	C6	C7	C9	C10	C12	C13	C14	C15	C16
Elevation above sea	[m]	279	275	287	293	282	275	252	297	277	251	229	278	239
Elevation above stream	[m]	11	10	9	2	4	8	4	8	7	6	10	10	10
Size	[ha]	48	12	18	65	110	47	288	336	544	700	1410	1913	6790
Lake	[%]	0	0	0	6	4	0	2	0	0	1	1	2	1
Forest	[%]	98	100	56	54	72	82	84	74	83	88	90	83	87
mire	[%]	2	0	44	40	24	18	14	26	17	10	5	14	9
Open land	[%]	0	0	0	0	0	0	0	0	0	0	1	1	1
Arable land	[%]	0	0	0	0	0	0	0	0	0	1	3	0	2
Tree volume ^a	[m ³ ha ⁻¹]	187	212	83	64	117	167	150	93	129	145	106	85	106
Land cover type ^b		forest	forest	mire	mire	mixed								

179 ^a Calculated for the entire catchment using correlations between a forest inventory (from 110 plots) and LiDAR measurements (Laudon et al.,
 180 2013).

181 ^b Landcover type was defined by percent mire coverage, with <2% mire as “forest”, 2-30% mire as “mixed”, and >30% mire as “mire”. C5 is
 182 the outlet to a headwater humic lake.

183 2.2 Environmental trends

184 ***Sulfate deposition.*** In late 1970s, S deposition reached its peak ($\sim 4 \text{ kg S ha}^{-1} \text{ yr}^{-1}$) in Krycklan.
185 Since 20 years ago, S deposition has consistently declined by snowfall and rainfall to less than 1
186 $\text{kg S ha}^{-1} \text{ yr}^{-1}$, and hence comparable to those observed during pre-industrial times (Laudon,
187 Sponseller, et al., 2021).

188 ***Temperature.*** The long-term air temperature record at Svartberget from 1980 to 2020 reveals a
189 clear pattern of overall warming. Since 1891, the annual air temperature has risen by
190 approximately $3.0 \text{ }^{\circ}\text{C}$. However, the most notable increase of $2.5 \text{ }^{\circ}\text{C}$ has occurred within the last
191 four decades, with 2020 standing out as the warmest year on record (Laudon, Hasselquist, et al.,
192 2021).

193 ***Precipitation.*** Over the last 40 years, there has been no statistical trend observed in the total
194 annual average precipitation, whereas a noticeable decrease has been observed in the average
195 duration of winter snow cover (Laudon, Hasselquist, et al., 2021).

196 ***Land use.*** In Krycklan, forestry is the dominating land use in the region, and most forests are
197 managed by conventional rotation forestry, including regeneration, thinning, and clear-cut
198 harvesting, resulting in a predomination of even-aged stands. On average, below 1% of the
199 catchment becomes clear-cut each year, but the most central catchments in Krycklan (C1, C2,
200 C4, C6, C7, C9) have been unmanaged for nearly a century (Figure S1).

201

202

203 2.3 Data collection & interpolation

204 ***Site characteristic.*** Catchment areas were delineated from a LiDAR derived digital elevation
205 model (DEM) and validated in the field using a professional mapper (Laudon et al., 2013). The
206 DEM with 2 m resolution was created from a point cloud with a point density of 15–25 points/m²
207 and hydrologically corrected by burning streams and culverts across roads (Lidberg et al., 2017).
208 The landscape type (forest, lake, and mire coverage) for each catchment was calculated
209 according to the Swedish property map (1:12,500, Lantmäteriet Gävle, Sweden) (Table 1).

210 ***Climate data.*** Air temperature and soil temperature at 20 cm were measured in the central part of
211 Krycklan at the Svartberget research station (Laudon, Hasselquist, et al., 2021). Climate data
212 from the station are assumed to be representative across the broader catchment area.

213 ***Chemistry data.*** Surface water samples were collected typically on the same day from each site
214 in acid-wash, high-density polyethylene bottles. The sampling frequency is every third day
215 during spring flood, biweekly during summer and fall, monthly in winter. All samples were
216 filtered immediately after collection (0.45µm MCE membrane, Millipore). DOC samples were
217 analyzed promptly after filtering to minimize any potential degradation or alteration of the
218 organic carbon compounds. DOC samples were run as soon as possible. DOC concentrations
219 were measured as total organic carbon (TOC) using a Shimadzu TOC-VCPH analyzer after
220 acidification to remove inorganic compounds (Laudon et al., 2011). DOC and TOC are
221 practically equivalent, so the term DOC is used in this study. Samples for sulfate were frozen
222 prior to analysis. Sulfate (SO₄) was measured by Dionex DX-300 or DX-320 ion
223 chromatography system (Fork et al., 2020). For more information about field sampling can be
224 found (Köhler et al., 2008; Laudon et al., 2013; Winterdahl et al., 2014). Daily DOC and SO₄

225 concentrations during 2003 to 2021 were interpolated using ‘*Random Forest*’ by package
226 ‘*missForest*’ (Stekhoven & Buhlmann, 2012) in R (R Core Team, 2019) (FigureS2).

227 **Discharge data.** Daily stream discharge of the 13 catchments during 2003 to 2021 were
228 predicted by an ensemble version of a bucket-type, semi-distributed hydrological (HBV) model
229 (Karimi et al., 2022). A more detailed description about the modeling part can be found in
230 Karimi et al., (2022).

231 **MODIS GPP data.** The gross primary productivity (GPP) derived from the Moderate Resolution
232 Imaging Spectroradiometer (MODIS) – hereafter MGPPP – is one of the most widely used GPP
233 products (X. Huang et al., 2021). Due to the absence of eddy covariance towers at each sub-
234 catchment, MGPP rather than eddy covariance GPP was applied as the agent of terrestrial
235 productivity in this study. Three methods were developed to extract MGPP (500 m and 8-day
236 resolution) from Google Earth Engine (Gorelick et al., 2017) according to the GIS data from
237 Krycklan database: 1) from the coordinate of each site (point); 2) from the riparian zone (50
238 meters on both side) of each catchment (line); 3) from the watershed of each site (area) (Figure
239 S2). Daily MGPP was linearly interpolated based on 8-day MGPP (Figure S3). To determine the
240 most representative MGPP, we compared MGPP and GPP derived from eddy-covariance at sites
241 where both estimates were available (Zhu et al., 2022). The results revealed that MGPP from
242 three different approaches accounted for 56% to 67% of the variability in eddy-covariance GPP
243 (Table S1). Among the three approaches, MGPP derived from the riparian zone exhibited the
244 highest explanatory power (R^2) (Table S2).

245

246

247 2.4 Statistical analysis

248 **Calculation of long-term trends.** For each site, the long-term trends of DOC concentrations (and
249 environmental drivers) during 2003-2021 were calculated as the slope of the simple linear
250 regression of mean values against the year. The mean slope of all catchments was used to
251 compute the long-term trend of each variable in the Krycklan catchment.

252 **Distributed-lag linear model.** The impact of each environmental factor to DOC concentrations
253 was quantified using distributed-lag linear models (DLMs), where the lag effect was applied to
254 discharge and MGPP according to the wavelet analysis described in Zhu et al. (2022). The cross-
255 basis of MGPP and discharge were built by polynomial transformations of the lags of MGPP and
256 discharge, respectively. In DLMs, fourth-degree polynomial cross-basis functions with 4-30 days
257 lag time were built for MGPP and second degree with 0-7 days for discharge (Zhu et al., 2022).
258 Then, linear combinations of SO₄, soil temperature, catchment size, mire coverage and the cross-
259 basis of discharge and MGPP were used to predict DOC concentrations. The analysis was
260 performed using the ‘DLNM’ package (Gasparrini, 2011) in R (R Core Team, 2019). The
261 Akaike information criterion (AIC) and R² were used to select the best model in predicting the
262 DOC concentrations. Finally, DLM 1-7 were defined as follows:

263

264

265

266

267

$$268 \quad DLM1: DOC = \beta_1 Dis_{lag} \quad (1)$$

$$269 \quad DLM2: DOC = \beta_1 MGPP_{lag} \quad (2)$$

$$270 \quad DLM3: DOC = \beta_1 Dis_{lag} + \beta_2 MGPP_{lag} \quad (3)$$

$$271 \quad DLM4: DOC = \beta_1 Dis_{lag} + \beta_2 MGPP_{lag} + \alpha_1 SO_4 \quad (4)$$

$$272 \quad DLM5: DOC = \beta_1 Dis_{lag} + \beta_2 MGPP_{lag} + \alpha_1 SO_4 + \alpha_2 T_{soil} \quad (5)$$

$$273 \quad DLM6: DOC = \beta_1 Dis_{lag} + \beta_2 MGPP_{lag} + \alpha_1 SO_4 + \alpha_2 T_{soil} + \alpha_3 Area \quad (6)$$

$$274 \quad DLM7: DOC = \beta_1 Dis_{lag} + \beta_2 MGPP_{lag} + \alpha_1 SO_4 + \alpha_2 T_{soil} + \alpha_3 Area + \alpha_4 Mire\% \quad (7)$$

275 Where β is the lag effect of discharge (Dis) and MGPP on DOC concentrations, α is the impact
 276 of sulfate (SO_4), soil temperature (T_{soil}), catchment size ($Area$) and mire coverage ($Mire\%$).
 277 Dis_{lag} and $MGPP_{lag}$ are the mean cross basis of discharge and MGPP during their lag times,
 278 respectively. In this study, we evaluated the performance of DLM2 when utilizing MGPP from
 279 three different methods. Our findings revealed that DLM2 performed the best when applying
 280 MGPP from the riparian zone, as it yielded the lowest AIC and highest R^2 values (Table S2).
 281 Thereafter, MGPP from the riparian zone was used for further analysis.

282 **Total differential equation.** To evaluate spatial patterns, we quantified the contributions of
 283 environmental drivers (sulfate, discharge, MGPP, soil temperature) to observed DOC trend
 284 during 2003-2021 across each site. This quantification was achieved by decomposing the 19-year
 285 linear trend of DOC in each site into the additive contributions of four components. To focus
 286 more on temporal patterns, we quantified the contributions of environmental drivers to 10-year
 287 DOC trend across each period. A 10-year moving window was used to cut the 19-year dataset at
 288 1-year interval to obtain 10 datasets (2003-2012, 2004-2013...& 2012-2021). Thereafter, we

289 decomposed the 10-year linear trend of DOC across each period into the additive contributions
 290 of four components.

$$\frac{d DOC}{dt} = \frac{\partial DOC}{\partial Dis} * \frac{d Dis}{dt} + \frac{\partial DOC}{\partial SO_4} * \frac{d SO_4}{dt} + \frac{\partial DOC}{\partial MGPP} * \frac{d MGPP}{dt} + \frac{\partial DOC}{\partial T_{soil}} * \frac{d T_{soil}}{dt}$$

$$291 = \Delta DOC^{Dis} + \Delta DOC^{SO_4} + \Delta DOC^{MGPP} + \Delta DOC^{T_{soil}} \quad (8)$$

292 where $\frac{\partial DOC}{\partial X}$ represents the sensitivity of *DOC* to an explanatory variable X --- sulfate (SO_4),
 293 discharge (*Dis*), soil temperature (T_{soil}) and *MGPP*. These sensitivities were estimated as the
 294 regression coefficients of a multiple linear regression performed with *DOC* against all listed
 295 explanatory variables at a certain period. $\frac{d DOC}{dt}$ (Or $\frac{dX}{dt}$) represents the linear trend of *DOC* (or X) at
 296 a certain period. For each site at a certain period, this trend was calculated as the slope of the
 297 simple linear regression of mean *DOC* (or X) values against the year. Here, The *DOC* trend at
 298 certain period ($\frac{d DOC}{dt}$) was decomposed into the contribution of each variable X (ΔDOC^X), which
 299 was represented as the product of the partial derivative against that variable X as $\frac{\partial DOC}{\partial X}$ and the
 300 concurrent trend of X itself as $\frac{dX}{dt}$. The approach given by Eq. (8) was conducted for each site, and
 301 the total areal-averaged contribution of each factor to the trend of *DOC* over each period was
 302 calculated by averaging the decomposed contribution of factors (ΔDOC^X) across all catchments.

303

304

305

306 **3. Results**

307 3.1 Long-term trends of DOC and environmental variables

308 The long-term trend analysis showed that DOC concentration did increase at each site over the
309 measured period. The mean DOC concentration trend (\pm s.d.) across the Krycklan catchments
310 was $0.22 \pm 0.11 \text{ mg l}^{-1} \text{ year}^{-1}$ ($p < 0.001$) (Figure 2a). Across all the catchments, the change was
311 significant ($p < 0.001$), whereas C2 had the steepest slope (0.38) and C5 had lowest (0.08) (Table
312 2). Overall, the small forest- dominated sites showed the highest rate of response ($0.38 \pm 0.04 \text{ mg}$
313 $\text{l}^{-1} \text{ year}^{-1}$, $n=2$), followed by the larger-size mixed catchments ($0.22 \pm 0.09 \text{ mg l}^{-1} \text{ year}^{-1}$, $n=9$),
314 whereas small-size mire catchments had the lowest rates ($0.09 \pm 0.004 \text{ mg l}^{-1} \text{ year}^{-1}$, $n=2$) (Table
315 2).

316 From 2003 to 2021, there were decreasing trends in SO_4 concentrations throughout all
317 catchments, with a mean trend of $-0.13 \pm 0.06 \text{ mg l}^{-1} \text{ year}^{-1}$ ($p < 0.001$) (Figure 2b). Among all
318 sites, C1 showed the steepest decline (-0.23) and C4 the lowest (-0.001). The declines in all sites
319 were significant ($p < 0.01$) except for C4 ($p = 0.95$) (Table 2). As with DOC changes, forest sites
320 had the largest declining trends (-0.22 ± 0.01 , $n=2$), followed by mixed (-0.13 ± 0.03 , $n=9$), while
321 mire outlet streams had the weakest trends (-0.02 ± 0.02 , $n=2$) (Table 2). Despite these trends of
322 declining SO_4 , stream pH at each site showed a declining trend from 2003 to 2021 with the mean
323 slope of $-0.02 \pm 0.01 \text{ year}^{-1}$ (Figure 2f). At 10 of the 13 catchments, the decline was statistically
324 significant ($p < 0.05$), while this not so ($p > 0.05$) at the other 3 sites (Table 2).

325 Other climatic and ecosystem variable show trends over the study period. For example, MGPP at
326 each catchment demonstrated an increasing trend from 2003 to 2021 with the mean slope of
327 $0.006 \pm 0.001 \text{ kg C m}^{-2} \text{ year}^{-1}$ (Figure 2c). The increase was significant ($p < 0.05$) at 5 of the 13

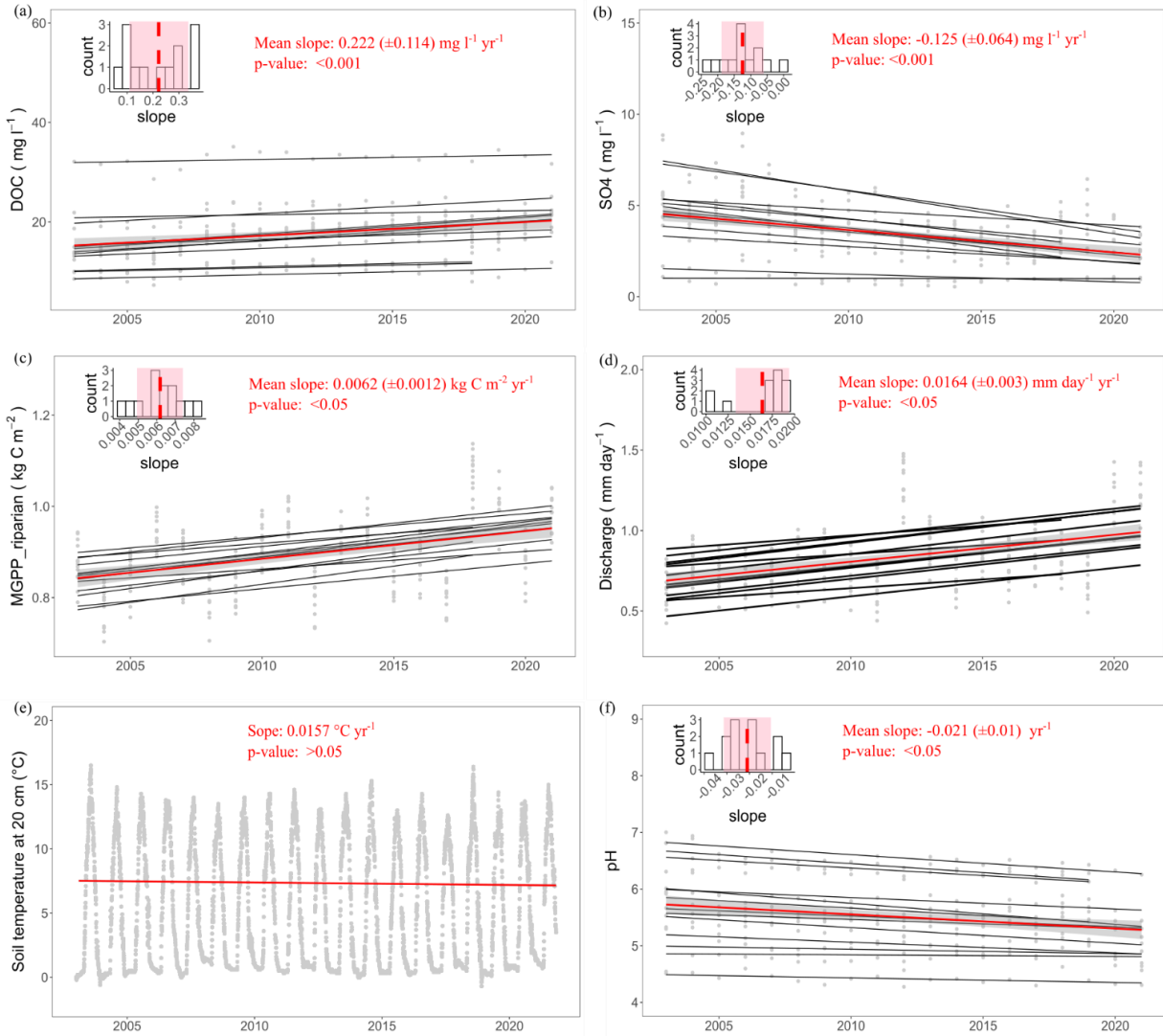
328 catchments (Table 2). Discharge at each site also displayed an increasing trend with mean slope
 329 of $0.02 \pm 0.003 \text{ mm day}^{-1} \text{ year}^{-1}$ in Krycklan (Figure 2d). It is important to note, these trends
 330 were strongly affected by the last two years of the record (Figure 2d). Nonetheless, at 10 of the
 331 13 catchments, the increase in discharge was statistically significant ($p < 0.05$), while this trend
 332 was positive but not significant ($p > 0.05$) at the other 3 sites (Table 2). Finally, soil temperature
 333 also showed a rising trend in the Krycklan with a slope of $0.016 \text{ }^\circ\text{C year}^{-1}$, but this was not
 334 statistically significant ($p > 0.05$) during 2003 to 2021 (Figure 2e). However, In C12, C14 and
 335 C15 (2003 to 2018) the soil temperature decreased (Table 2).

336 Table 2. The long-term trends of DOC concentrations, MODIS GPP (MGPP), discharge, sulfate, soil temperature
 337 and stream pH from 2003 to 2021 across sites. The measured period is 2003 to 2018 in C12, C14 and C15.

Site	Size (ha)	Land cover	DOC		MGPP		Discharge		Sulfate		Soil temperature		Stream pH	
			Slope	p-values	Slope	p-values	Slope	p-values	Slope	p-values	Slope ^a	p-values	Slope	p-values
C1	48	forest	0.371	<0.001	0.006	NS	0.018	<0.05	-0.234	<0.001	0.016	NS	-0.015	<0.05
C2	12	forest	0.378	<0.001	0.006	NS	0.018	<0.05	-0.206	<0.001	0.016	NS	-0.019	<0.01
C4	18	mire	0.090	<0.001	0.006	NS	0.019	<0.05	-0.001	NS	0.016	NS	-0.008	NS
C5	65	mire	0.082	<0.001	0.004	NS	0.019	<0.05	-0.042	<0.01	0.015	NS	-0.003	NS
C6	110	mixed	0.174	<0.001	0.006	<0.05	0.019	<0.05	-0.082	<0.01	0.016	NS	-0.019	<0.05
C7	47	mixed	0.278	<0.001	0.006	<0.05	0.018	<0.05	-0.132	<0.001	0.016	NS	-0.008	NS
C9	288	mixed	0.215	<0.001	0.005	NS	0.018	<0.05	-0.126	<0.001	0.016	NS	-0.020	<0.01
C10	336	mixed	0.282	<0.001	0.007	<0.05	0.017	<0.05	-0.115	<0.001	0.016	NS	-0.028	<0.01
C12	544	mixed	0.309	<0.001	0.004	NS	0.011	NS	-0.184	<0.001	-0.006	NS	-0.026	<0.05
C13	700	mixed	0.366	<0.001	0.007	<0.05	0.017	<0.05	-0.134	<0.001	0.016	NS	-0.037	<0.001
C14	1410	mixed	0.110	<0.001	0.008	NS	0.011	NS	-0.157	<0.001	-0.006	NS	-0.027	<0.01
C15	1913	mixed	0.121	<0.001	0.008	NS	0.012	NS	-0.123	<0.001	-0.006	NS	-0.032	<0.001
C16	6790	mixed	0.113	<0.001	0.007	<0.05	0.017	<0.05	-0.083	<0.01	0.016	NS	-0.031	<0.001

338 ^aSoil temperature trends in C12, C14 and C15 were from 2003 to 2018 to match DOC data, as records from 2018 to 2021 were missing at these

339 three sites.



340

341 Figure 2. The long-term trends of DOC concentration (a), SO_4 (b), MGPP(c), discharge (d), soil temperature at 20cm
 342 (e) and stream pH (f) in Krycklan from 2003 to 2021. The annual changes of all variables were calculated using
 343 daily data across all sites. The red line represents the mean trend across all sites over 19 years. The grey area
 344 highlights trends within one standard deviation of the mean trend. Individual site observations and trends are given
 345 as grey points and black lines, respectively. The inset shows the distribution of the rate of change in DOC across the
 346 Krycklan catchment. Dashed red line represents the mean slope. The red shaded area represents the mean slope \pm
 347 standard deviation.

348

349

350 3.2 Environmental drivers of DOC variations

351 The inclusion of more environmental factors in the analysis resulted in an improvement of the
352 performance of DLMs, indicated by the increase in R^2 and decrease in AIC. DLM7 ($DOC =$
353 $\beta_1 Dis_{lag} + \beta_2 MGPP_{lag} + \alpha_1 SO_4 + \alpha_2 T_{soil} + \alpha_3 Area + \alpha_4 Mire\%$) was the best-performing
354 model among all the DLMs, which explained 53 % of DOC concentrations across 13 catchments
355 in Krycklan (Table 3).

356 According to DLM7, the contributions of all environmental drivers under different proposed
357 mechanisms controlling DOC concentrations were quantified. During 2003-2021, recovery of
358 SO_4 deposition was the dominant mechanism accounting for 31% of DOC concentrations, with
359 the climate change mechanism contributing 6.9%. There was also important spatial
360 heterogeneity, with site characteristics also playing a crucial role in regulating DOC
361 concentrations, explaining 15% (Figure 3).

362 Specifically, sulfate and catchment size were the most important drivers and inversely correlated
363 with DOC concentrations (Table S3), explaining 31% and 13% respectively (Figure 3).
364 Thereafter, discharge, MGPP, mire coverage and soil temperature accounted for 4%, 3%, 2% and
365 0.2% of the DOC variation, respectively (Figure 3). Among these, mire coverage and soil
366 temperature contributed positively to DOC concentrations. However, the contributions of MGPP
367 and discharge to DOC were more complex, could be either positive or negative (Table S3).

368

369

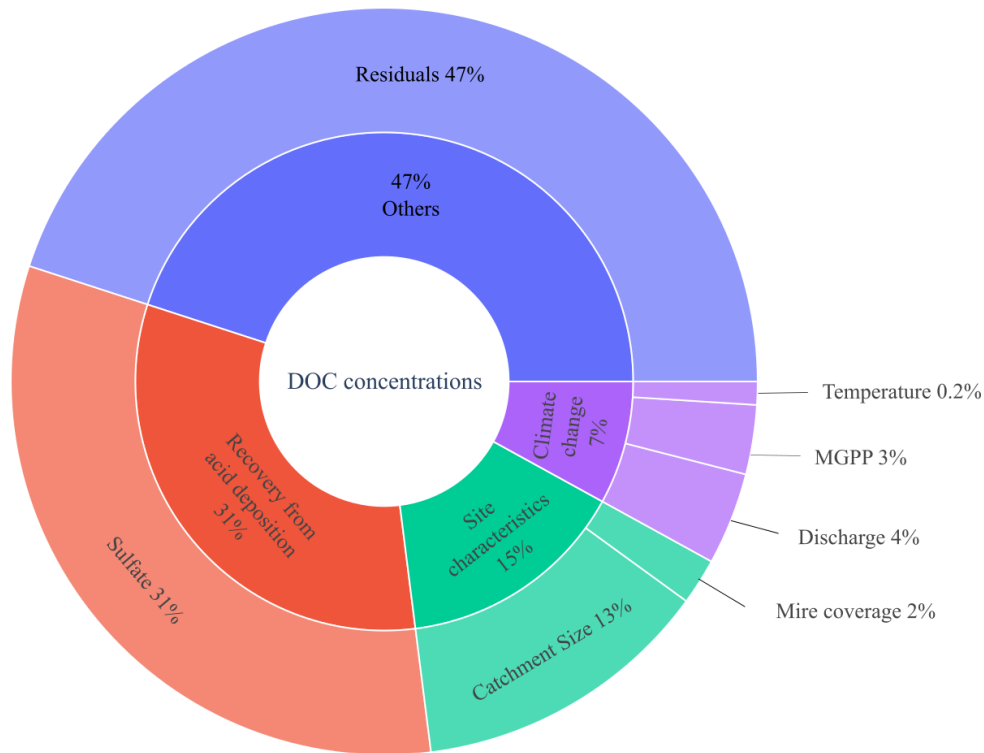
370

371 Table 3. Performances of distributed-lag linear models (DLMs) show the relationship between dissolved organic
 372 carbon (DOC) variations and potential environmental drivers across 13 boreal catchments in Krycklan. $MGPP_{lag}$
 373 means the cross basis of MODIS GPP from riparian zone; DIS_{lag} represents the cross basis of discharge; T_{soil} is soil
 374 temperature at 20cm; *Area* means catchment size. *Mire%* is the proportion of mire according to the landscape of
 375 catchment.

Distributed-lag linear Models (DLMs)	Discharge		MGPP		Performance	
	Lag/day	Degree	Lag/day	Degree	AIC	R ²
1. DOC= DIS_{lag}	0–7	2	-	-	241681.3	0.04
2. DOC= $MGPP_{lag}$	-	-	4–30	4	243021.7	0.02
3. DOC= $DIS_{lag} + MGPP_{lag}$	0–7	2	4–30	4	239037.2	0.07
4. DOC= $DIS_{lag} + MGPP_{lag} + SO_4$	0–7	2	4–30	4	203457.9	0.38
5. DOC= $DIS_{lag} + MGPP_{lag} + SO_4 + T_{soil}$	0–7	2	4–30	4	202970.3	0.38
6. DOC= $DIS_{lag} + MGPP_{lag} + SO_4 + T_{soil} + Area$	0–7	2	4–30	4	183503.3	0.51
7. DOC= $DIS_{lag} + MGPP_{lag} + SO_4 + T_{soil} + Area + Mire\%$	0–7	2	4–30	4	179979.3	0.53

376

377



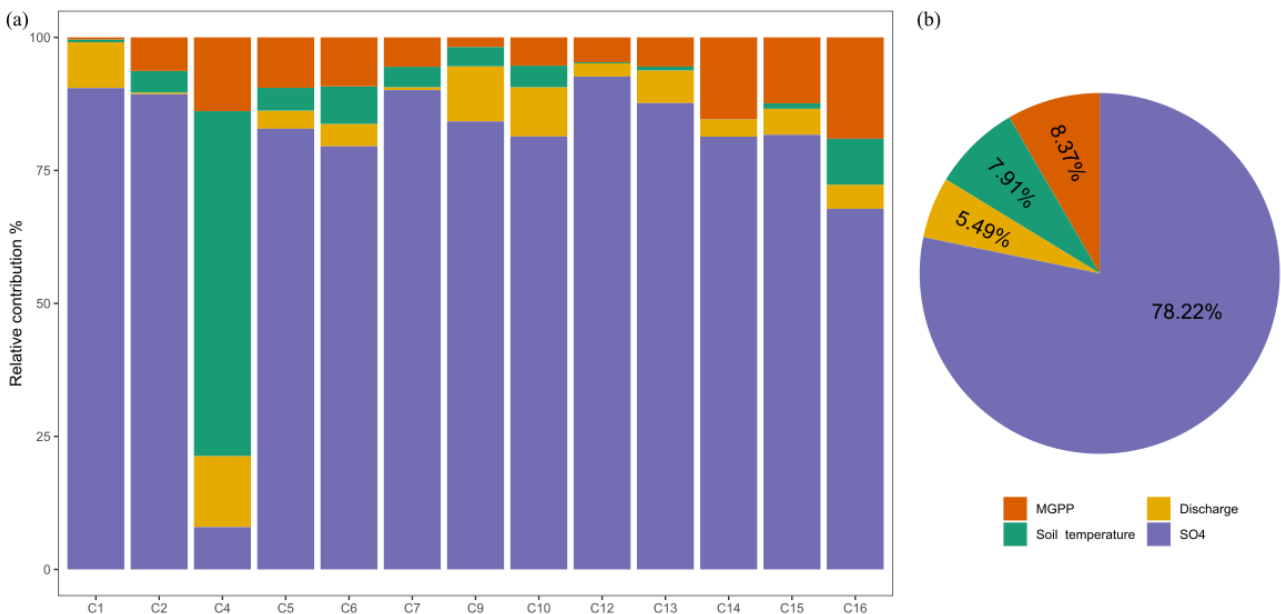
378

379 Figure 3. The contribution of proposed mechanisms and site characteristics to the variation of DOC concentrations

380 in Krycklan catchments during 2003-2021 according to the best distributed-lag linear model (DLM7).

381 3.3 Attributions of long-term DOC trends in spatial scale

382 By the total differential equation, we attributed the long-term increased DOC trends of all
 383 Krycklan catchments from 2003 to 2021 to four environmental drivers. However, the
 384 contributions of the drivers varied across catchments (Figure 4a). For 12 of the 13 sites, SO₄ was
 385 the dominant driver of the long-term (19 years) trends of increasing DOC. In fact, only for C4
 386 (mire site) soil temperature was the most crucial factor (Figure 4a). In 9 of the 13 catchments, the
 387 subsequent important contributor was MGPP, whereas at the other 4 sites discharge played this
 388 secondary role (Figure 4a). In summary, SO₄ was the main factor controlling the long-term trend
 389 of DOC in Krycklan, followed by MGPP, temperature, and discharge during the study period
 390 (Figure 4b).

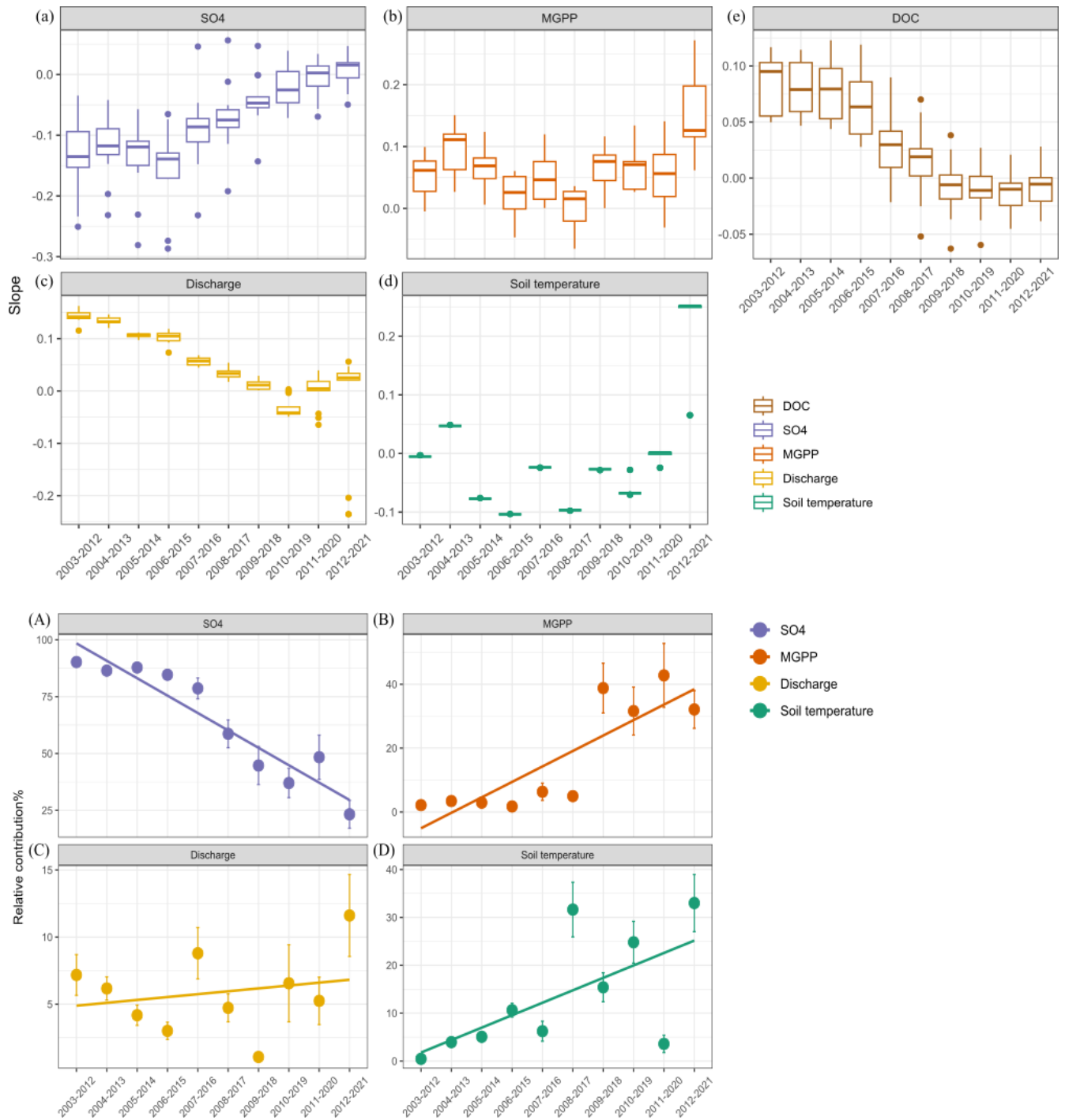


391
 392 Figure 4. The relative contribution (%) of each driver to long-term DOC trends across 13 catchments in Krycklan
 393 during 2003-2021 (a). The mean relative contribution of each driver to long-term DOC trend in Krycklan during
 394 2003-2021 (b).

395

396 3.4 Attributions of long-term DOC trends in temporal scale

397 A 10-year moving window from 2003 to 2021 created 10 sets of 10-year long sequences to test
398 the trend variations in DOC and all environmental variables temporally (Figure 5). The slopes of
399 DOC decreased from the decade in early 2000s to the last decade which indicated the upward
400 trend of DOC slowed down or even ceased in the most recent years (Figure 5e). From the first
401 decade to the last, the decreasing trend of SO_4 became smaller and then leveled off entirely
402 (Figure 5a). The rising trends of discharge also moderated with time (Figure 5c). The slopes of
403 MGPP and soil temperature were relatively stable during the first 9 periods but increased in the
404 last decade (Figure 5b & d). The trends of DOC over different periods were also attributed to the
405 trends exhibited by environmental drivers using differential equations (Figure 5). The influence
406 of SO_4 reduced (Figure 5A) while the contributions of MGPP (Figure 5B) and soil temperature
407 (Figure 5D) in controlling long-term DOC trends increased. Whereas the contributions of
408 discharge to long-term DOC trends were stable during all the periods (Figure 5C).

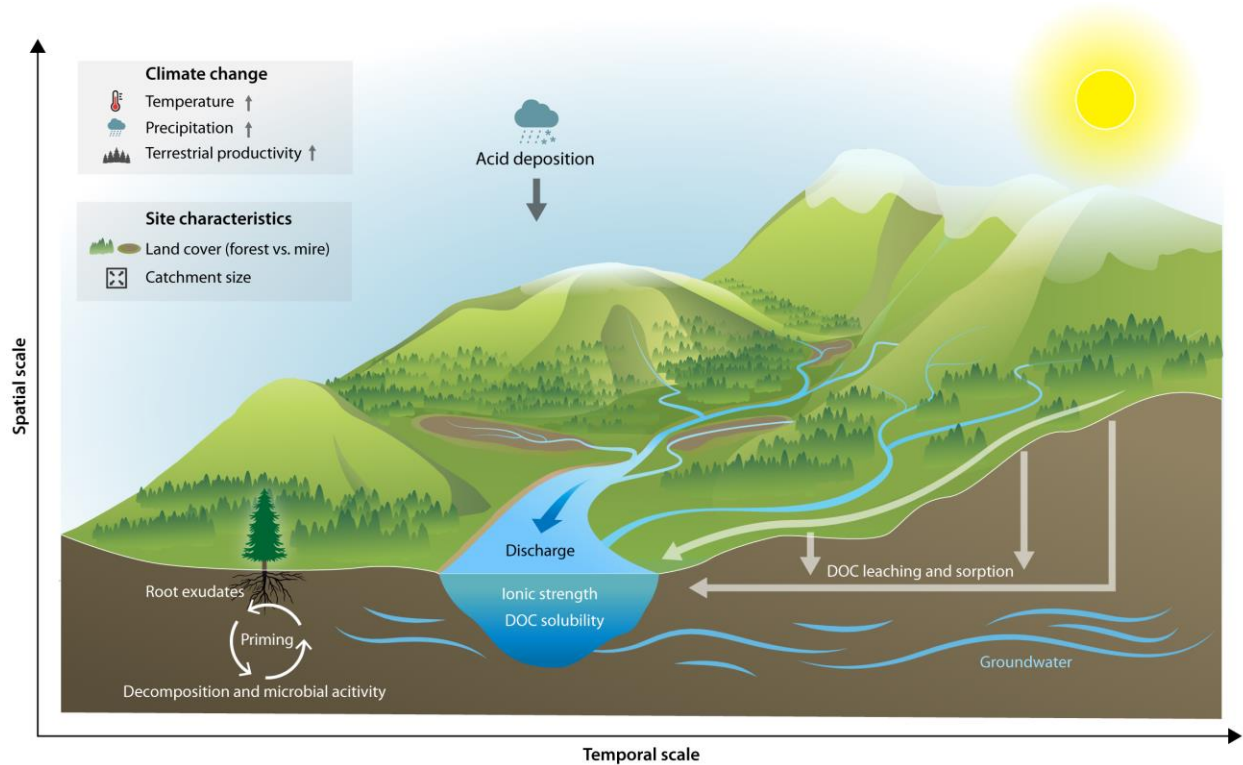


409

410 Figure 5. The slope of sulfate (SO₄) (a), MODIS GPP (MGPP) (b), discharge (c), soil temperature (d) and DOC
 411 trend (e) across all the periods (10-year moving window from 2003 to 2021) in Krycklan catchments. Meanwhile,
 412 the relative contribution (%) of SO₄ (A), MGPP (B), discharge (C) and soil temperature (D) to long-term DOC
 413 trends across all the periods.

414 **4. Discussion**

415 Over the period from 2003 to 2021, all catchments in Krycklan experienced an increasing trend
416 in DOC concentrations, although these upward trends varied among sites. Our study indicated
417 that no single mechanism could account for the entire variation in DOC trends over space and
418 time. Instead, we showed that a combination of factors, including sulfate deposition, terrestrial
419 productivity (with delay), discharge (with delay), soil temperature, and properties of the
420 catchment such as size and land cover type govern the dynamic of DOC trends. When
421 considering all sites together, the primary drivers of the long-term DOC trend (spanning 19
422 years) were the concurrent declines in stream sulfate concentrations, followed by increases in
423 terrestrial productivity, soil temperature, and discharge (Figure 6). Additionally, DOC trends
424 varied in magnitude by five-fold across sub-catchments within the Krycklan network,
425 highlighting a major role for catchment properties (landcover and sizes) as modulators of stream
426 response to environmental change (Figure 6). Briefly, the increase in long-term DOC
427 concentrations was more pronounced in catchments with higher forest and lower mire cover
428 (open peatland) (i.e., forest > mixed > mire sites), but the rate of increase tended to slow down
429 from smaller to larger catchments.



430

431 Figure 6. Conceptual diagram illustrating the mechanisms (Acid deposition, climate change and site characteristics)
 432 of browning across a boreal catchment network, spanning two-decades. DOC means dissolved organic carbon.

433 Whereas our modeling approach identified multiple drivers of DOC variations, stream SO_4
 434 concentrations emerged as by far the most important (Figure 3). This mechanism is supported by
 435 the first order control that declining stream SO_4 concentrations exerted over the long-term DOC
 436 trends (Figure 4b). Furthermore, such observations are consistent with past studies in Krycklan
 437 that have assessed DOC- SO_4 relationships in soil water (Ledesma et al., 2016). S-deposition can
 438 alter DOC solubility by changing either the acidity of soils or (and) the ionic strength of soil
 439 solutions (Monteith et al., 2007). In contrast to expectation, annual pH has not recovered during
 440 the study period, but instead has declined slightly at all sites (Figure 2f). Thus, we suggest that
 441 the rise in DOC and associated organic acidity, overwhelm the trends in S-deposition from the
 442 standpoint of stream pH (Laudon et al., 2021b). Strikingly, the Krycklan streams have witnessed

443 a large decline also in the sum of base cations (BC), primarily Ca and Mg, that in a charge
444 perspective are comparable to the decline in SO₄ concentration (Laudon et al., 2021b). This
445 concurrent decrease in SO₄ and BC decreased ionic strength, which consequently enhanced the
446 colloidal dispersion and organic matter disaggregation in soil solution by expanding the diffuse
447 double layer. Such changes, in turn, can increase the solubility of DOC in soil water and promote
448 its lateral export to streams (Lawrence & Roy, 2021). Therefore, the decline in ionic strength
449 rather than recovery from acidification seems to be the main driver of the increasing DOC trends
450 across Krycklan catchments. It is noteworthy that the large DOC trends occurred despite the
451 relatively low sulfate deposition in Krycklan, peaking at 4 kg S ha⁻¹ yr⁻¹ around 1980 (Laudon et
452 al., 2021b), more than 5 times lower compared to the most affected parts of Sweden (Ferm et al.,
453 2019).

454 Our results also revealed important impacts of climate related factors, including increases in
455 forest productivity and changes in discharge. Previous studies have also linked increasing
456 production and mobilization of terrestrial organic C from soils to browning (Finstad et al., 2016).
457 There have been apparent increases in forest growth in and around the Krycklan Catchment
458 throughout the last 60 years (Laudon, Hasselquist, et al., 2021), and this trend has likely
459 increased the size of soil organic matter pools that can be mobilized to streams (Jansson et al.,
460 2008). Further, previous work in Krycklan revealed the lag-effects of terrestrial productivity on
461 soil DOC production through priming (Zhu et al., 2022), while the current study confirmed these
462 findings across a larger number of catchments and over an extended period. Finally, while the
463 relationship between increasing discharge and elevated DOC concentrations is in line with theory
464 (Wit et al., 2016), this pattern should be interpreted with caution as the discharge time series is
465 weighted by the final two years in the record. Indeed, there is increasing evidence that

466 hydrological patterns in northern landscapes are becoming more variable with climate change
467 (Teutschbein & Seibert, 2012) and that more severe summer droughts in the Krycklan can have
468 large influences on DOC, with lower concentrations during low flow, followed by elevated
469 concentrations during rewetting phases (Tiwari et al., 2022). Regardless, our analysis illustrates
470 how multiple, climate-related features can operate concurrently with deposition recovery to
471 shape stream DOC trends.

472 Landcover type can further regulate the patterns between discharge, SO_4 , terrestrial productivity
473 and DOC concentrations. Firstly, there is substantial heterogeneity in the hydrological pathways
474 that connect soils and streams for different landscapes (Laudon & Sponseller, 2018). For sites
475 with high mire cover, a larger proportion of water travels overland due to frozen surfaces or
476 within deeper preferential flow paths that can be diluted during high flows (Peralta-Tapia et al.,
477 2015a). By comparison, runoff from forest hillslopes enters streams through subsurface flow
478 pathways could carry newly activated soil organic C to the catchment (Laudon et al., 2004).
479 Therefore, more DOC is flushed into streams draining forest catchments, while dilution is more
480 common for mire catchments, resulting in decreasing concentrations during rain events (Bishop
481 et al., 2004). This may account for the fact that, despite similar discharge patterns across
482 catchments during the study period (Figure 2d), the response rates of DOC were higher in sites
483 with greater forest cover. Simultaneously, imported SO_4 to the mire sites has also been washed
484 out and diluted because of much higher hydrological connectivity and greater contribution of
485 overland flow (Peralta-Tapia et al., 2015a). Additionally, mires are known to promote sulphate
486 reduction processes (Pester et al., 2012) as persistent anaerobic conditions allow sulphate-
487 reducing bacteria to convert SO_4 to sulfide, removing SO_4 from the system (Porowski et al.,
488 2019; Taketani et al., 2010). Thus, we observed lower mean concentrations (Figure S4) and

489 weaker trends for SO_4 (Table 2) in sites with higher mire coverage. Our results highlighted the
490 dilution and buffer function of mires, such that greater peat coverage dampen the response rate of
491 DOC to sulfate deposition. Moreover, the terrestrial productivity and stand biomass increased
492 with higher forest and lower mire cover, which led to higher load of fresh organic matter from
493 terrestrial to aquatic ecosystem, consequently higher response rate of DOC concentrations
494 (Crapart et al., 2023).

495 Meanwhile, catchment size can also regulate DOC response rates through changes in the
496 dominant water pathways supporting stream flow. Accordingly, for larger catchments, the
497 contribution of deeper, DOC-poor groundwater to streams is usually greater, reducing the
498 significance of DOC inputs from near-surface soils that are dominant sources in the headwaters
499 (Shanley et al., 2002; Strohmenger et al., 2021; Peralta-Tapia et al., 2015b). This hydrological
500 pattern appears widespread in the region (Tiwari et al., 2018), and the increasing supply of
501 deeper groundwater likely buffers against changes in DOC mobilization that are generated in
502 shallower soils. By modifying the importance of different water sources, increased catchment
503 sizes could moderate the response of DOC to environmental drivers.

504 Among the more novel results from our analysis is the resolution of non-stationary drivers of
505 DOC export over time. The observed decline in browning across Krycklan catchments aligns
506 with the findings of Eklöf et al., (2021) who showed that increases in DOC that were prevalent
507 throughout Sweden during 1991-2010 ended a decade ago. The fact that browning trends have
508 weakened during the last ten years in Krycklan suggested that recovery from sulfate deposition
509 was strong in the early 2000s, but not throughout the second decade (Figure 5a). Despite this, as
510 the significance of changes in SO_4 concentration diminished over time, the relative importance of
511 terrestrial productivity and soil temperature increased (Figure 5). Yet, the absolute contributions

512 of these factors to DOC trends should remain roughly consistent, suggesting that these emergent
513 drivers are considerably weaker in their capacity to elevate stream DOC when compared to the
514 deposition recovery response. Indeed, the contribution of terrestrial productivity to variations in
515 DOC concentrations can be either positive or negative, according to the direction of priming
516 effect under different landscapes and C inputs (Zhu et al., 2022). Meanwhile, the contributions of
517 discharge across time were relatively stable despite the shift importance of the other drivers.
518 Although soil temperature made a relatively greater contribution during the last decade, it is
519 unlikely to generate a substantial upward trend of DOC alone (Freeman et al., 2001; Pastor et al.,
520 2003). Therefore, without the strong driving force of sulfate, other factors are likely insufficient
521 to maintain the long-term trend.

522 While DOC trends in the Krycklan appear to be leveling off, ongoing browning observed at other
523 sites in Sweden can be attributed to either the influence of land use changes (Lindbladh et al.,
524 2014; Kritzberg, 2017; Škerlep et al., 2020) or to deposition recovery at locations that received
525 far higher inputs, particularly in the south, from which catchments may take a longer time to
526 recover (Eklöf et al., 2021). Yet the patterns we observe in this more northern landscape largely
527 concur with Evans et al., (2006), in that rising DOC in freshwaters can to a large extent reflect
528 recovery from sulfate deposition, and thus future predictions of dramatic intensification of C
529 export from terrestrial ecosystem may perhaps be overly pessimistic, at least in the short term.
530 Indeed, we acknowledged that the different variables we evaluated likely trigger stream DOC
531 responses at very different time scales. For example, the effects of changing SO_4 and temperature
532 on DOC mobilization seems almost instantaneous, whereas the effects of building up a larger
533 humus layer from elevated terrestrial productivity could result in a DOC increases decades later.
534 These long-term cumulative responses are much more difficult to capture so far.

535

536 **5. Conclusion**

537 Our study provides evidence that large (five-fold) variation in browning trends among northern
538 streams can reflect the outcome of interactions among multiple factors, including recovery from
539 sulfate deposition, climate-related factors, and catchment properties. Our results further suggest
540 that recovery from sulfate rather than from acidification *per se* has been the main driver of DOC
541 change, despite the low deposition history in this region. Additionally, our modeling approach
542 revealed the important lag-effects of terrestrial production and discharge on stream DOC, albeit
543 with weaker influences on overall DOC trends when compared to SO₄ declines. That also led to
544 the fact that browning has weakened in the last decade, as stream sulfate levels have plummeted
545 while other drivers were insufficient to sustain the ongoing long-term trend of DOC.

546

547

548

549

550

551

552

553

554

555

556 **Acknowledgments**

557 This work was funded by Kone project (201906598) - ‘The role of terrestrial productivity on
558 fluxes of DOC in watersheds (Maaekosysteemien tuottavuuden merkitys liukoisen orgaanisen
559 hiilen virtoihin valuma-alueilla)’ and partly by UEF Water (The water research program has
560 received a special endowment from Olvi Foundation, Jenny and Antti Wihuri Fund, and
561 Saastamoinen Foundation). We thank the funders of the Krycklan Catchment Study, including
562 the Swedish Infrastructure for Ecosystem Science (SITES), The Kempe foundation, the VR
563 extreme event project, and the Swedish Research Council for Sustainable Development
564 (FORMAS).

565

566

567 **Data Availability Statement**

568 The water chemistry, hydrological data, climate data and GIS data used in this study are
569 available from Krycklan Data Portal via www.slu.se/Krycklan.

570

571

572

573

574

575 **References**

- 576 Aitkenhead, J. A., & McDowell, W. H. (2000). Soil C:N ratio as a predictor of annual riverine
577 DOC flux at local and global scales. *Global Biogeochemical Cycles*, *14*(1), 127–138.
578 <https://doi.org/10.1029/1999GB900083>
- 579 Bishop, K., Seibert, J., Köhler, S., & Laudon, H. (2004). Resolving the Double Paradox of
580 rapidly mobilized old water with highly variable responses in runoff chemistry.
581 *Hydrological Processes*, *18*(1), 185–189. <https://doi.org/10.1002/hyp.5209>
- 582 Blanchet, C. C., Arzel, C., Davranche, A., Kahilainen, K. K., Secondi, J., Taipale, S., et al.
583 (2022). Ecology and extent of freshwater browning - What we know and what should be
584 studied next in the context of global change. *Science of The Total Environment*, *812*,
585 152420. <https://doi.org/10.1016/j.scitotenv.2021.152420>
- 586 Ciais, P., Schelhaas, M. J., Zaehle, S., Piao, S. L., Cescatti, A., Liski, J., et al. (2008). Carbon
587 accumulation in European forests. *Nature Geoscience*, *1*(7), 425–429.
588 <https://doi.org/10.1038/ngeo233>
- 589 Clark, J. M., Bottrell, S. H., Evans, C. D., Monteith, D. T., Bartlett, R., Rose, R., et al. (2010).
590 The importance of the relationship between scale and process in understanding long-term
591 DOC dynamics. *Science of The Total Environment*, *408*(13), 2768–2775.
592 <https://doi.org/10.1016/j.scitotenv.2010.02.046>
- 593 Cole, J. J., Prairie, Y. T., Caraco, N. F., McDowell, W. H., Tranvik, L. J., Striegl, R. G., et al.
594 (2007). Plumbing the Global Carbon Cycle: Integrating Inland Waters into the Terrestrial
595 Carbon Budget. *Ecosystems*, *10*(1), 172–185. <https://doi.org/10.1007/s10021-006-9013-8>

- 596 Conley, D. J., Carstensen, J., Aigars, J., Axe, P., Bonsdorff, E., Eremina, T., et al. (2011).
597 Hypoxia Is Increasing in the Coastal Zone of the Baltic Sea. *Environmental Science &*
598 *Technology*, 45(16), 6777–6783. <https://doi.org/10.1021/es201212r>
- 599 Crapart, C., Finstad, A. G., Hessen, D. O., Vogt, R. D., & Andersen, T. (2023). Spatial predictors
600 and temporal forecast of total organic carbon levels in boreal lakes. *Science of The Total*
601 *Environment*, 870, 161676. <https://doi.org/10.1016/j.scitotenv.2023.161676>
- 602 Drake, T. W., Raymond, P. A., & Spencer, R. G. M. (2018). Terrestrial carbon inputs to inland
603 waters: A current synthesis of estimates and uncertainty. *Limnology and Oceanography*
604 *Letters*, 3(3), 132–142. <https://doi.org/10.1002/lol2.10055>
- 605 Driscoll, C. T., Fuller, R. D., & Simone, D. M. (1988). Longitudinal Variations in Trace Metal
606 Concentrations in a Northern Forested Ecosystem. *Journal of Environmental Quality*,
607 17(1), 101–107. <https://doi.org/10.2134/jeq1988.00472425001700010015x>
- 608 Eklöf, K., von Brömssen, C., Amvrosiadi, N., Fölster, J., Wallin, M. B., & Bishop, K. (2021).
609 Brownification on hold: What traditional analyses miss in extended surface water records.
610 *Water Research*, 203, 117544. <https://doi.org/10.1016/j.watres.2021.117544>
- 611 Evans, C., Chapman, P., Clark, J. M., Monteith, D., & Cresser, M. S. (2006). Alternative
612 explanations for rising dissolved organic carbon export from organic soils. *Global*
613 *Change Biology*, 12, 2044–2053. <https://doi.org/10.1111/J.1365-2486.2006.01241.X>
- 614 Ferm, M., Granat, L., Engardt, M., Pihl Karlsson, G., Danielsson, H., Karlsson, P. E., & Hansen,
615 K. (2019). Wet deposition of ammonium, nitrate and non-sea-salt sulphate in Sweden
616 1955 through 2017. *Atmospheric Environment: X*, 2, 100015.
617 <https://doi.org/10.1016/j.aeoa.2019.100015>

- 618 Finstad, A. G., Andersen, T., Larsen, S., Tominaga, K., Blumentrath, S., de Wit, H. A., et al.
619 (2016a). From greening to browning: Catchment vegetation development and reduced S-
620 deposition promote organic carbon load on decadal time scales in Nordic lakes. *Scientific*
621 *Reports*, 6(1), 31944. <https://doi.org/10.1038/srep31944>
- 622 Finstad, A. G., Andersen, T., Larsen, S., Tominaga, K., Blumentrath, S., de Wit, H. A., et al.
623 (2016b). From greening to browning: Catchment vegetation development and reduced S-
624 deposition promote organic carbon load on decadal time scales in Nordic lakes. *Scientific*
625 *Reports*, 6(1), 31944. <https://doi.org/10.1038/srep31944>
- 626 Fork, M. L., Sponseller, R. A., & Laudon, H. (2020). Changing Source-Transport Dynamics
627 Drive Differential Browning Trends in a Boreal Stream Network. *Water Resources*
628 *Research*, 56(2), e2019WR026336. <https://doi.org/10.1029/2019WR026336>
- 629 Freeman, C., Evans, C. D., Monteith, D. T., Reynolds, B., & Fenner, N. (2001). Export of
630 organic carbon from peat soils. *Nature*, 412(6849), 785–785.
631 <https://doi.org/10.1038/35090628>
- 632 Futter, M. N., & de Wit, H. A. (2008). Testing seasonal and long-term controls of streamwater
633 DOC using empirical and process-based models. *Science of The Total Environment*,
634 407(1), 698–707. <https://doi.org/10.1016/j.scitotenv.2008.10.002>
- 635 Gasparrini, A. (2011). Distributed Lag Linear and Non-Linear Models in R: The Package dlnm.
636 *Journal of Statistical Software*, 43(1), 1–20. <https://doi.org/10.18637/jss.v043.i08>
- 637 Gorelick, N., Hancher, M., Dixon, M., Ilyushchenko, S., Thau, D., & Moore, R. (2017). Google
638 Earth Engine: Planetary-scale geospatial analysis for everyone. *Remote Sensing of*
639 *Environment*, 202, 18–27. <https://doi.org/10.1016/j.rse.2017.06.031>

- 640 Härkönen, L. H., Lepistö, A., Sarkkola, S., Kortelainen, P., & Räike, A. (2023). Reviewing
641 peatland forestry: Implications and mitigation measures for freshwater ecosystem
642 browning. *Forest Ecology and Management*, *531*, 120776.
643 <https://doi.org/10.1016/j.foreco.2023.120776>
- 644 Hongve, D., Riise, G., & Kristiansen, J. F. (2004). Increased colour and organic acid
645 concentrations in Norwegian forest lakes and drinking water – a result of increased
646 precipitation? *Aquatic Sciences*, *66*(2), 231–238. [https://doi.org/10.1007/s00027-004-](https://doi.org/10.1007/s00027-004-0708-7)
647 [0708-7](https://doi.org/10.1007/s00027-004-0708-7)
- 648 Huang, X., Xiao, J., Wang, X., & Ma, M. (2021). Improving the global MODIS GPP model by
649 optimizing parameters with FLUXNET data. *Agricultural and Forest Meteorology*, *300*,
650 108314. <https://doi.org/10.1016/j.agrformet.2020.108314>
- 651 Jansson, M., Hickler, T., Jonsson, A., & Karlsson, J. (2008). Links between Terrestrial Primary
652 Production and Bacterial Production and Respiration in Lakes in a Climate Gradient in
653 Subarctic Sweden. *Ecosystems*, *11*(3), 367–376. [https://doi.org/10.1007/s10021-008-](https://doi.org/10.1007/s10021-008-9127-2)
654 [9127-2](https://doi.org/10.1007/s10021-008-9127-2)
- 655 Karimi, S., Seibert, J., & Laudon, H. (2022). Evaluating the effects of alternative model
656 structures on dynamic storage simulation in heterogeneous boreal catchments. *Hydrology*
657 *Research*, *53*(4), 562–583. <https://doi.org/10.2166/nh.2022.121>
- 658 Karlsson, J., Byström, P., Ask, J., Ask, P., Persson, L., & Jansson, M. (2009). Light limitation of
659 nutrient-poor lake ecosystems. *Nature*, *460*, 506–509.
660 <https://doi.org/10.1038/nature08179>
- 661 Keller, W. (Bill), Paterson, A. M., Somers, K. M., Dillon, P. J., Heneberry, J., & Ford, A. (2008).
662 Relationships between dissolved organic carbon concentrations, weather, and

- 663 acidification in small Boreal Shield lakes. *Canadian Journal of Fisheries and Aquatic*
664 *Sciences*, 65(5), 786–795. <https://doi.org/10.1139/f07-193>
- 665 Köhler, S. J., Buffam, I., Laudon, H., & Bishop, K. H. (2008). Climate’s control of intra-annual
666 and interannual variability of total organic carbon concentration and flux in two
667 contrasting boreal landscape elements. *Journal of Geophysical Research: Biogeosciences*,
668 113(G3). <https://doi.org/10.1029/2007JG000629>
- 669 Kritzberg, E. S. (2017). Centennial-long trends of lake browning show major effect of
670 afforestation. *Limnology and Oceanography*, 2, 105–112.
671 <https://doi.org/10.1002/LOL2.10041>
- 672 Kritzberg, E. S., Hasselquist, E. M., Škerlep, M., Löfgren, S., Olsson, O., Stadmark, J., et al.
673 (2020). Browning of freshwaters: Consequences to ecosystem services, underlying
674 drivers, and potential mitigation measures. *Ambio*, 49(2), 375–390.
675 <https://doi.org/10.1007/s13280-019-01227-5>
- 676 Lapierre, J.-F., Collins, S. M., Oliver, S. K., Stanley, E. H., & Wagner, T. (2021). Inconsistent
677 browning of northeastern U.S. lakes despite increased precipitation and recovery from
678 acidification. *Ecosphere*, 12(3), e03415. <https://doi.org/10.1002/ecs2.3415>
- 679 Larsen, S., Andersen, T., & Hessen, D. O. (2011). Predicting organic carbon in lakes from
680 climate drivers and catchment properties. *Global Biogeochemical Cycles*, 25(3).
681 <https://doi.org/10.1029/2010GB003908>
- 682 Laudon, H., & Sponseller, R. A. (2018). How landscape organization and scale shape catchment
683 hydrology and biogeochemistry: insights from a long-term catchment study. *WIREs*
684 *Water*, 5(2), e1265. <https://doi.org/10.1002/wat2.1265>

- 685 Laudon, H., Köhler, S., & Buffam, I. (2004). Seasonal TOC export from seven boreal
686 catchments in northern Sweden. *Aquatic Sciences - Research Across Boundaries*, 66(2),
687 223–230. <https://doi.org/10.1007/s00027-004-0700-2>
- 688 Laudon, H., Berggren, M., Ågren, A., Buffam, I., Bishop, K., Grabs, T., et al. (2011). Patterns
689 and Dynamics of Dissolved Organic Carbon (DOC) in Boreal Streams: The Role of
690 Processes, Connectivity, and Scaling. *Ecosystems*, 14(6), 880–893.
691 <https://doi.org/10.1007/s10021-011-9452-8>
- 692 Laudon, H., Taberman, I., Ågren, A., Futter, M., Ottosson-Löfvenius, M., & Bishop, K. (2013).
693 The Krycklan Catchment Study—A flagship infrastructure for hydrology,
694 biogeochemistry, and climate research in the boreal landscape. *Water Resources*
695 *Research*, 49(10), 7154–7158. <https://doi.org/10.1002/wrcr.20520>
- 696 Laudon, H., Hasselquist, E. M., Pechl, M., Lindgren, K., Sponseller, R., Lidman, F., et al.
697 (2021a). Northern landscapes in transition: Evidence, approach and ways forward using
698 the Krycklan Catchment Study. *Hydrological Processes*, 35(4), e14170.
699 <https://doi.org/10.1002/hyp.14170>
- 700 Laudon, H., Sponseller, R. A., & Bishop, K. (2021b). From legacy effects of acid deposition in
701 boreal streams to future environmental threats. *Environmental Research Letters*, 16(1),
702 015007. <https://doi.org/10.1088/1748-9326/abd064>
- 703 Lawrence, G. B., & Roy, K. M. (2021). Ongoing increases in dissolved organic carbon are
704 sustained by decreases in ionic strength rather than decreased acidity in waters recovering
705 from acidic deposition. *Science of The Total Environment*, 766, 142529.
706 <https://doi.org/10.1016/j.scitotenv.2020.142529>

- 707 Leach, T. H., Winslow, L. A., Hayes, N. M., & Rose, K. C. (2019). Decoupled trophic responses
708 to long-term recovery from acidification and associated browning in lakes. *Global*
709 *Change Biology*, 25(5), 1779–1792. <https://doi.org/10.1111/gcb.14580>
- 710 Ledesma, J. L. J., Futter, M. N., Laudon, H., Evans, C. D., & Köhler, S. J. (2016). Boreal forest
711 riparian zones regulate stream sulfate and dissolved organic carbon. *Science of The Total*
712 *Environment*, 560–561, 110–122. <https://doi.org/10.1016/j.scitotenv.2016.03.230>
- 713 Lepistö, A., Räike, A., Sallantausta, T., & Finér, L. (2021). Increases in organic carbon and
714 nitrogen concentrations in boreal forested catchments — Changes driven by climate and
715 deposition. *Science of The Total Environment*, 780, 146627.
716 <https://doi.org/10.1016/j.scitotenv.2021.146627>
- 717 Lidberg, W., Nilsson, M., Lundmark, T., & Ågren, A. M. (2017). Evaluating preprocessing
718 methods of digital elevation models for hydrological modelling. *Hydrological Processes*,
719 31(26), 4660–4668. <https://doi.org/10.1002/hyp.11385>
- 720 Lindbladh, M., Axelsson, A.-L., Hultberg, T., Brunet, J., & Felton, A. (2014). From broadleaves
721 to spruce – the borealization of southern Sweden. *Scandinavian Journal of Forest*
722 *Research*, 29(7), 686–696. <https://doi.org/10.1080/02827581.2014.960893>
- 723 Martell, A. E., Motekaitis, R. J., & Smith, R. M. (1988). Structure-stability relationships of
724 metal complexes and metal speciation in environmental aqueous solutions.
725 *Environmental Toxicology and Chemistry*, 7(6), 417–434.
726 <https://doi.org/10.1002/etc.5620070603>
- 727 Monteith, D. T., Stoddard, J. L., Evans, C. D., de Wit, H. A., Forsius, M., Høgåsen, T., et al.
728 (2007). Dissolved organic carbon trends resulting from changes in atmospheric
729 deposition chemistry. *Nature*, 450(7169), 537–540. <https://doi.org/10.1038/nature06316>

- 730 Myers-Smith, I. H., Kerby, J. T., Phoenix, G. K., Bjerke, J. W., Epstein, H. E., Assmann, J. J., et
731 al. (2020). Complexity revealed in the greening of the Arctic. *Nature Climate Change*,
732 *10*(2), 106–117. <https://doi.org/10.1038/s41558-019-0688-1>
- 733 Mzobe, P., Berggren, M., Pilesjö, P., Lundin, E., Olefeldt, D., Roulet, N. T., & Persson, A.
734 (2018). Dissolved organic carbon in streams within a subarctic catchment analysed using
735 a GIS/remote sensing approach. *PLOS ONE*, *13*(7), e0199608.
736 <https://doi.org/10.1371/journal.pone.0199608>
- 737 Pagano, T., Bida, M., & Kenny, J. E. (2014). Trends in Levels of Allochthonous Dissolved
738 Organic Carbon in Natural Water: A Review of Potential Mechanisms under a Changing
739 Climate. *Water*, *6*(10), 2862–2897. <https://doi.org/10.3390/w6102862>
- 740 Pastor, J., Solin, J., Bridgham, S. D., Updegraff, K., Harth, C., Weishampel, P., & Dewey, B.
741 (2003). Global warming and the export of dissolved organic carbon from boreal peatlands.
742 *Oikos*, *100*(2), 380–386. <https://doi.org/10.1034/j.1600-0706.2003.11774.x>
- 743 Peralta-Tapia, A., Sponseller, R. A., Tetzlaff, D., Soulsby, C., & Laudon, H. (2015a).
744 Connecting precipitation inputs and soil flow pathways to stream water in contrasting
745 boreal catchments. *Hydrological Processes*, *29*(16), 3546–3555.
746 <https://doi.org/10.1002/hyp.10300>
- 747 Peralta-Tapia, Andrés, Sponseller, R. A., Ågren, A., Tetzlaff, D., Soulsby, C., & Laudon, H.
748 (2015b). Scale-dependent groundwater contributions influence patterns of winter
749 baseflow stream chemistry in boreal catchments. *Journal of Geophysical Research:*
750 *Biogeosciences*, *120*(5), 847–858. <https://doi.org/10.1002/2014JG002878>
- 751 Pester, M., Knorr, K.-H., Friedrich, M., Wagner, M., & Loy, A. (2012). Sulfate-reducing
752 microorganisms in wetlands – fameless actors in carbon cycling and climate change.

- 753 *Frontiers in Microbiology*, 3. Retrieved from
754 <https://www.frontiersin.org/articles/10.3389/fmicb.2012.00072>
- 755 Porowski, A., Porowska, D., & Halas, S. (2019). Identification of Sulfate Sources and
756 Biogeochemical Processes in an Aquifer Affected by Peatland: Insights from Monitoring
757 the Isotopic Composition of Groundwater Sulfate in Kampinos National Park, Poland.
758 *Water*, 11(7), 1388. <https://doi.org/10.3390/w11071388>
- 759 R Core Team. (2019). *R: A Language and Environment for Statistical Computing*. Vienna,
760 Austria: R Foundation for Statistical Computing. Retrieved from [https://www.R-](https://www.R-project.org/)
761 [project.org/](https://www.R-project.org/)
- 762 Räike, A., Kortelainen, P., Mattsson, T., & Thomas, D. N. (2016). Long-term trends (1975–2014)
763 in the concentrations and export of carbon from Finnish rivers to the Baltic Sea: organic
764 and inorganic components compared. *Aquatic Sciences*, 78(3), 505–523.
765 <https://doi.org/10.1007/s00027-015-0451-2>
- 766 Redden, D., Trueman, B. F., Dunnington, D. W., Anderson, L. E., & Gagnon, G. A. (2021).
767 Chemical recovery and browning of Nova Scotia surface waters in response to declining
768 acid deposition. *Environmental Science: Processes & Impacts*, 23(3), 446–456.
769 <https://doi.org/10.1039/D0EM00425A>
- 770 Schlesinger, W. H., & Andrews, J. A. (2000). Soil respiration and the global carbon cycle.
771 *Biogeochemistry*, 48(1), 7–20. <https://doi.org/10.1023/A:1006247623877>
- 772 Shanley, J. B., Kendall, C., Smith, T. E., Wolock, D. M., & McDonnell, J. J. (2002). Controls on
773 old and new water contributions to stream flow at some nested catchments in Vermont,
774 USA. *Hydrological Processes*, 16(3), 589–609. <https://doi.org/10.1002/hyp.312>

- 775 Škerlep, M., Steiner, E., Axelsson, A.-L., & Kritzberg, E. S. (2020). Afforestation driving long-
776 term surface water browning. *Global Change Biology*, 26(3), 1390–1399.
777 <https://doi.org/10.1111/gcb.14891>
- 778 Stekhoven, D. J., & Buhlmann, P. (2012). MissForest--non-parametric missing value imputation
779 for mixed-type data. *Bioinformatics*, 28(1), 112–118.
780 <https://doi.org/10.1093/bioinformatics/btr597>
- 781 Strohmenger, L., Fovet, O., Hrachowitz, M., Salmon-Monviola, J., & Gascuel-Oudou, C. (2021).
782 Is a simple model based on two mixing reservoirs able to reproduce the intra-annual
783 dynamics of DOC and NO₃ stream concentrations in an agricultural headwater catchment?
784 *Science of The Total Environment*, 794, 148715.
785 <https://doi.org/10.1016/j.scitotenv.2021.148715>
- 786 Taketani, R. G., Yoshiura, C. A., Dias, A. C. F., Andreote, F. D., & Tsai, S. M. (2010). Diversity
787 and identification of methanogenic archaea and sulphate-reducing bacteria in sediments
788 from a pristine tropical mangrove. *Antonie van Leeuwenhoek*, 97(4), 401–411.
789 <https://doi.org/10.1007/s10482-010-9422-8>
- 790 Teutschbein, C., & Seibert, J. (2012). Bias correction of regional climate model simulations for
791 hydrological climate-change impact studies: Review and evaluation of different methods.
792 *Journal of Hydrology*, 456–457, 12–29. <https://doi.org/10.1016/j.jhydrol.2012.05.052>
- 793 Tiwari, T., Sponseller, R. A., & Laudon, H. (2018). Extreme Climate Effects on Dissolved
794 Organic Carbon Concentrations During Snowmelt. *Journal of Geophysical Research:
795 Biogeosciences*, 123(4), 1277–1288. <https://doi.org/10.1002/2017JG004272>

- 796 Tiwari, T., Sponseller, R. A., & Laudon, H. (2022). The emerging role of drought as a regulator
797 of dissolved organic carbon in boreal landscapes. *Nature Communications*, *13*(1), 5125.
798 <https://doi.org/10.1038/s41467-022-32839-3>
- 799 Tranvik, L. J., & Jansson, M. (2002). Terrestrial export of organic carbon. *Nature*, *415*(6874),
800 861–862. <https://doi.org/10.1038/415861b>
- 801 Winterdahl, M., Erlandsson, M., Futter, M. N., Weyhenmeyer, G. A., & Bishop, K. (2014). Intra-
802 annual variability of organic carbon concentrations in running waters: Drivers along a
803 climatic gradient. *Global Biogeochemical Cycles*, *28*(4), 451–464.
804 <https://doi.org/10.1002/2013GB004770>
- 805 Wit, H. A., Valinia, S., Weyhenmeyer, G., Futter, M., Kortelainen, P., Austnes, K., et al. (2016).
806 Current Browning of Surface Waters Will Be Further Promoted by Wetter Climate.
807 *Environmental Science and Technology Letters*, *3*, 430–435.
808 <https://doi.org/10.1021/ACS.ESTLETT.6B00396>
- 809 Zhu, X., Chen, L., Pumpanen, J., Ojala, A., Zobitz, J., Zhou, X., et al. (2022). The role of
810 terrestrial productivity and hydrology in regulating aquatic dissolved organic carbon
811 concentrations in boreal catchments. *Global Change Biology*, *28*(8).
812 <https://doi.org/10.1111/gcb.16094>

**Several mechanisms drive the heterogeneity in browning
across a boreal stream network**

Xudan Zhu¹, Frank Berninger¹, Liang Chen¹, Johannes Larson², Ryan A. Sponseller³, Hjalmar Laudon²

¹Department of Environmental and Biological Sciences, Joensuu Campus, University of Eastern Finland, 80100 Joensuu, Finland.

²Department of Forest Ecology and Management, Swedish University of Agricultural Science, 90183 Umeå, Sweden.

³ Department of Ecology and Environmental Sciences, Umeå University, 901 87 Umeå, Sweden.

Corresponding author: Xudan Zhu (xudanzhu@uef.fi).

Contents of this file

Tables S1 to S3

Figures S1 to S4

Introduction

This document contains additional information on the modeling outputs (Table S1-S3), clearcut records (Figure S1), conceptual diagram of MODIS GPP extraction (Figure S2), daily data interpolations (Figure S3) and mean chemical data across sites (Figure S4).

Table S1. The relationship between gross primary productivity derived from eddy-covariance measurements (EC GPP) and MODIS GPP (MGPP) extracted by three methods) in C2, C4 and C6. MGPP_coordinate means MGPP extracted from coordinate, MGPP_riparian represents MGPP extracted from riparian zone, while MGPP_watershed is MGPP extracted from the watershed. EC GPP are from Svartberget and Degerö station.

Sites (EC towers)	EC GPP~MGPP_coordinate		EC GPP~MGPP_riparian		EC GPP~MGPP_watershed	
	R ²	p-value	R ²	p-value	R ²	p-value
C2 (Svartberget)	0.565	<0.001	0.665	<0.001	0.565	<0.001
C4 (Degerö)	0.557	<0.001	0.656	<0.001	0.567	<0.001
C6 (Svartberget)	0.561	<0.001	0.660	<0.001	0.576	<0.001

Table S2. The performance of distributed-lag linear model (DLM2: $DOC = \beta_1 MGPP_{lag}$) with MODIS GPP (MGPP) from three different methods. MGPP_coordinate means MGPP extracted from coordinate, MGPP_riparian represents MGPP extracted from riparian zone, while MGPP_watershed is MGPP extracted from the watershed.

DLM2	Lag\day	AIC	R ²
DOC=MGPP_coordinate _{lag}	4–30	243156.9	0.020
DOC= MGPP_riparian _{lag}	4–30	243021.7	0.022
DOC= MGPP_watershed _{lag}	4–30	243076.8	0.021

Table S3. Coefficients table of DLM7 ($DOC \sim DIS_{lag} + MGPP_{lag} + SO_4 + T_{soil} + Area + Mire\%$). MGPP_{lag} means the cross basis of MODIS GPP from riparian zone; DIS_{lag} represents the cross basis of discharge; T_{soil} is soil temperature at 20cm; Area means the size of catchment. Wetland% is the proportion of wetland according to the landcover of catchment. cb.dis1, cb.dis2 and cb.dis3 are the second-degree polynomial cross basis of discharge, while cb.MGPP1, cb.MGPP2 and cb.MGPP3 are the fourth-degree polynomial cross basis of MGPP. Signif. codes: < 0.001 '***', < 0.01 '**', < 0.05 '*', >0.05 'NS'.

Index	Estimate	Std. Error	t value	Pr(> t)	
(Intercept)	-0.0950314	0.0053484	-17.768	< 0.001	***
cb.dis1	0.0735426	0.003605	20.4	< 0.001	***
cb.dis2	-0.271298	0.0224589	-12.08	< 0.001	***
cb.dis3	0.2156376	0.0222629	9.686	< 0.001	***
cb.MGPP1	-0.2823892	0.0361552	-7.81	< 0.001	***
cb.MGPP2	2.0973512	0.3549015	5.91	< 0.001	***
cb.MGPP3	-5.1436045	1.1318383	-4.544	< 0.001	***
cb.MGPP4	5.0050337	1.4433395	3.468	< 0.001	***
cb.MGPP5	-1.6310001	0.6359909	-2.565	< 0.05	*
SO ₄	-0.365123	0.0033677	-108.42	< 0.001	***
T _{soil}	0.1348511	0.0067255	20.051	< 0.001	***
Area	-0.0187109	0.0001348	-138.854	< 0.001	***
Mire%	0.0164285	0.000273	60.182	< 0.001	***

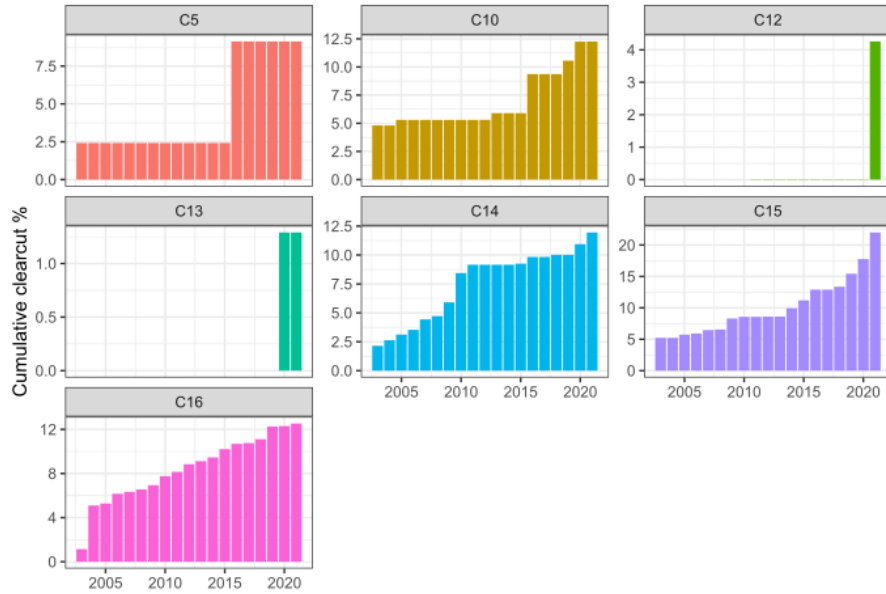


Figure S1. The cumulative clearcut proportion across sites with clearcutting during 2003 to 2021 in Krycklan. C16 is the outlet of Krycklan catchments, therefore represent clearcut record of the whole Krycklan. The annual clearcut proportion of Krycklan is 1%.

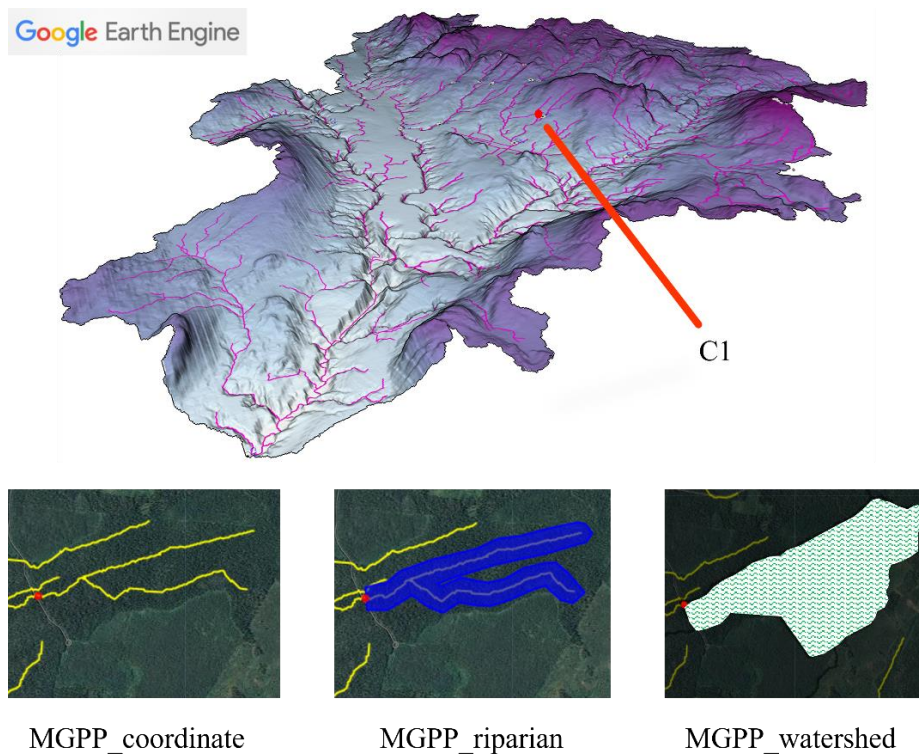


Figure S2. Schematic for extract MODIS GPP (MGPP) from coordinate, riparian zone and watershed of each site in Google Earth Engine

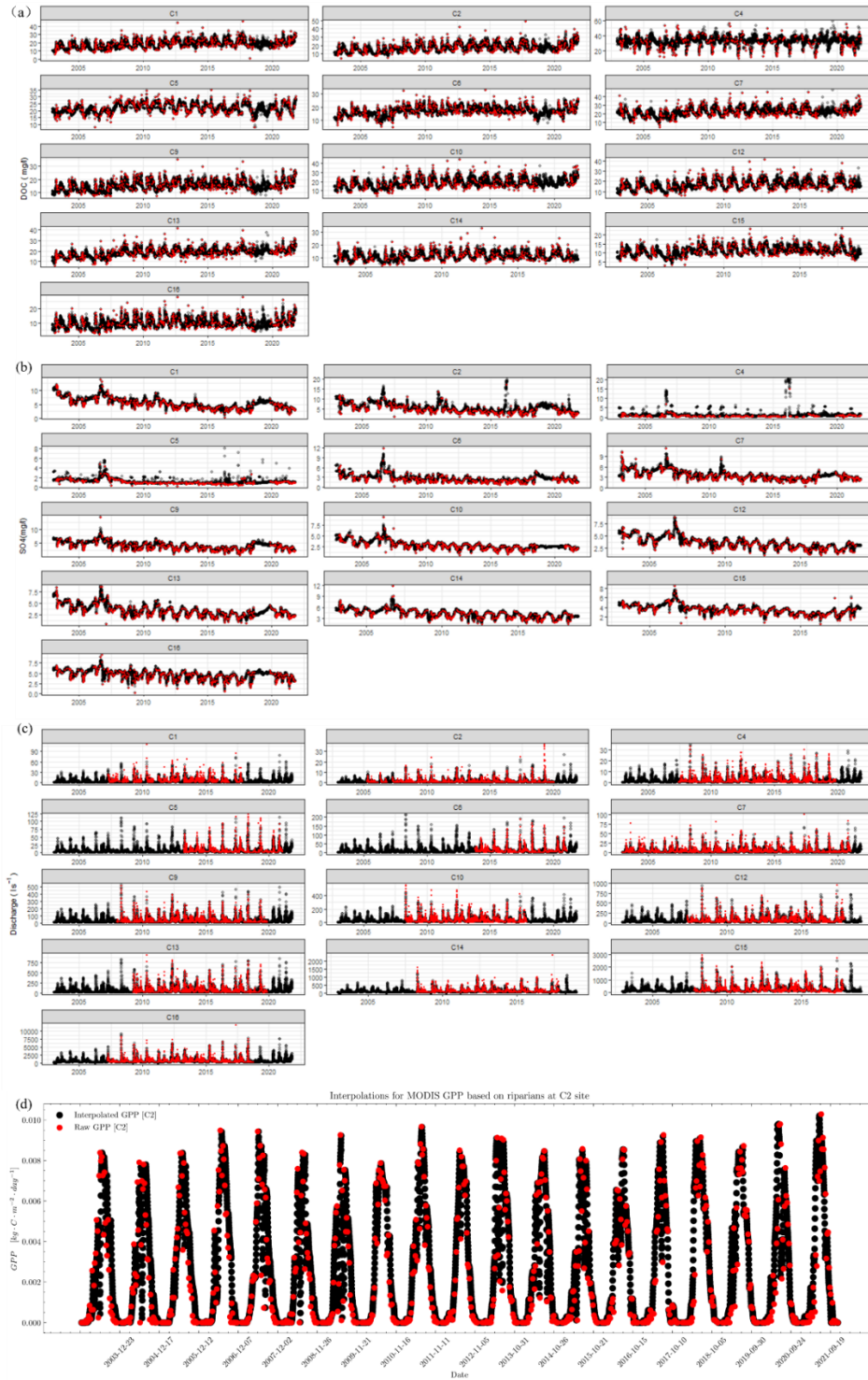


Figure S3. The raw observations vs interpolated daily data in DOC (a), SO₄(b), Discharge (c) and MODIS GPP (d). Individual observations are given as red dots, while the interpolated data are shown as black dots. Daily DOC and SO₄were interpolated by Random Forest; Daily Discharge was predicted by an ensemble version of a bucket-type, semi-distributed hydrological model (HBV); Daily MODIS GPP was gap filled linearly according to 8-day MODIS GPP.

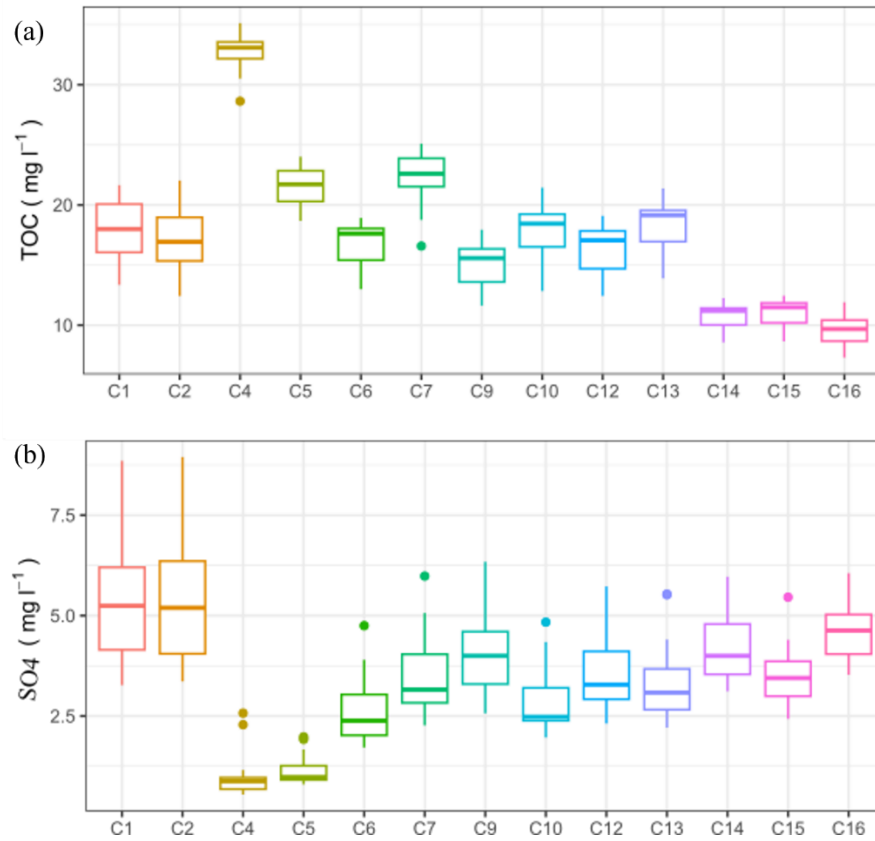


Figure S4. The mean DOC (a) and SO₄ (b) concentrations during 2003 to 2021 across catchments in Krycklan.